Thermo-Economic Optimization of Slim Well Power Cycles: A Case of Ngozi Geothermal Project-Tanzania

John Joseph Lubuva

Thesis of 60 ECTS credits

Master of Science (M.Sc.) in Sustainable Energy Engineering

Iceland School of Energy

October 2021

THERMO-ECONOMIC OPTIMIZATION OF SLIM WELL POWER CYCLES: A CASE OF NGOZI GEOTHERMAL PROJECT-TANZANIA

John Joseph Lubuva

Thesis of 60 ECTS credit submitted to the School of Science and Engineering a Reykjavik University in partial fulfilment of the requirements for the degree of

Master of Science in Sustainable Energy Engineering -

Iceland School of Energy

October 2021

Student:

John Lubuva

Supervisors:

Guðrún Arnbjörg Sævarsdóttir

Vijay Chauhan

Examiner:

María S. Guðjónsdóttir

The undersigned hereby grants permission to the Reykjavík University Library to reproduce single copies of this Thesis entitled **Thermo-economic Optimization of Slim Well Power Cycles: A Case of Ngozi Geothermal Project-Tanzania** and to lend or sell such copies for private, scholarly, or scientific research purposes only.

The author reserves all other publication and other rights in association with the copyright in the Thesis, and except as herein before provided, neither the Thesis nor any substantial portion thereof may be printed or otherwise reproduced in any material form whatsoever without the author's prior written permission.

20/10/2021

Date

J. Lubuva

John Joseph Lubuva
Master of Science

Thermo-economic Optimization of Slim Well Power Cycles: A Case of Ngozi Geothermal Project- Tanzania.

John Joseph Lubuva

October 2021

Abstract

Ngozi geothermal field located in Mbeya Tanzania, is the main geothermal project that the country focuses on, aiming at producing clean energy in term of both electricity and heat. The project is an exploration drilling phase.

The present study focuses on developing an optimized strategy in terms of wellbore size selection and power plant technology to be used, for the development of Ngozi geothermal field in Tanzania. To obtain this, a comparative thermo-economic analysis of slim wells against full size wells is done for a selection of power plant cycles. To obtain a realistic estimate of the wellbore output, as required for the thermo-economic analysis, well bore data from Pritchett [1] is used as basis for the analysis. The geothermal field is assumed to be liquid dominated.

Results show that, binary cycle has the highest first and second law efficiencies, produces the highest net-work output, and offers the lowest total cost per unit Megawatt compared to single and double flash power cycles. The binary technology would therefore be the most suitable power plant technology to be employed in Ngozi geothermal prospect. Apart from the capability to produce the highest amount net-work output and lowest cost per unit megawatt compared to the other slim wellbore diameters, the well can support testing.

If a geothermal field is liquid dominated and low enthalpy, slim wells would be more suitable for the power production instead of full-size wells. It can be concluded that in liquid dominated, low enthalpy geothermal fields, where a decision is to be made to drill slim wells, 15 cm well bore diameter slim wells are more suitable. It has also been shown that it takes less time to break even when slim wells are used to produce power compared to full size wells.

The results from this work are expected to equip developers including TGDC with adequate information to approach exploration drilling with a holistic and strategic view of minimizing the total investment cost and using exploration slim holes more productively compared to the traditional way. The aim is to improve energy efficiency and prove the business case for start-up geothermal projects with production taking place after drilling and testing successful slim wells instead of just plugging them. Moreover, to use slim well for production, proper casing design must be used to allow the flow of adequate quantity of geothermal fluids for production of electricity.

Varmahagfræðileg bestun á orkuferli grannra rannsóknarholna: könnun á jarðhitaverkefninu í Ngozi – Tansaníu

John Joseph Lubuva

Október 2021

Útdráttur

Ngozi jarðhitasvæðið, sem er í Mbeya í Tanzaníu, er helsta jarðhitaverkefni á dagskrá hjá Tanzanískum stjórnvöldum, með það í huga að auka framboð endurnýjanlegrar orku, bæði raforku og varma. Verkefnið er nú í könnunarfasa.

Í þessari meistararitgerð er þróuð aðferðafræði til að velja hagkvæmustu og áhættuminnstu tæknina, bæði hvað varðar borholugerð og vinnuhring, til að vinna orku frá Ngozi jarðhitasvæðinu. Með þetta að markmiði, var gerð varmahagfræðileg samanburðargreining á grönnum könnunarholum (e: slim wells) og hefðbundnum jarðhitaboroholum, fyrir nokkrar gerðir af vinnuhringjum. Byggt var á borholugögnum frá Pritchett [1] til að meta rennsli, holutoppsþrýsting og vermi jarðhitavökvans fyrir mismunandi holugerðir, sem forsendu fyrir hermanir á vinnuhringjunum, en þau gögn voru fyrir jarðhitasvæði með fremur lágt vermi, líkt og búist er við í Ngozi.

Í ljós kom að binary vinnuhringur hefur bestu fyrsta og annars lögmáls nýtni, skilar mestri vinnu og lægsta kostnaðaverði pr. Megawatt af uppsettu afli, í samanburði við opnar gufuhringrásir með einu eða tveimur þrýstingsþrepum. Binary vinnuhringur væri því hagkvæmasta tæknin fyrir jarðhitavirkjun á Ngozi svæðinu.

Fyrir jarðhitasvæði með tiltölulega lágt vermi jarðhitavökva er hagkvæmara að nota grannar könnunarholur (slim wells) til orkuvinnslu heldur en hefðbundnar vinnsluholur. Niðurstöður líkansins benda til þess að hagkvæmast sé að bora holur með 15 cm þvermáli, sem könnunarholur, sem síðan má nýta sem vinnsluholur. Sýnt er fram á að virkjunin borgar sig upp á styttri tíma þegar grannar holur eru notaðar í stað hefðbundinna vinnsluhola.

Telja má að lærdómurinn frá þessu verkefni muni nýtast TGDC og framkvæmdaaðila í Ngozi til ákvarðanatöku og veita fullnægjandi heildarmynd til að unnt verði að lágmarka áhættu, og fjárfestingakostnað með því að nýta grannar könnunarholur í könnunarfasanum, og jafnframt til framleiðslu, og þar með útvíkka og framlengja hlutverk þeirra í virkjuninni.

Markmiðið er að bæta orkunýtnina og sýna fram á hagkvæmni þess fyrir jarðhitavirkjanir í framkvæmdafasa að hefja strax framleiðslu frá vel heppnuðum grönnum könnunarholum í stað þess að loka þeim og bora nýjar vinnsluholur. Til að þetta sé mögulegt er mikilvægt að velja rétt hannaða fóðringu til að fá nægjanlegt rennsli jarðhitavökva frá holunni til orkuvinnslu.

Acknowledgements

TABLE OF CONTENT

List of tables

List of figures

Nomenclature

$\dot{C}$ = cost rate in $/s

c = cost per unit exergy in $/kJ

E = exergy rate in kW

$\dot{Z}$ = Investment Cost rate in $/s

$\dot{Q}$ = rate of heat transferred

U = heat transfer coefficient

A = area of heat exchanger

SCFM = Standard Cubic Feet per Minute

ACFM = Actual Cubic Feet per Minute

η_{th} = thermal or first law efficiency

$T_{re\text{-}injection}$ = re-injection temperature

$\dot{m}_1$ = mass flow rate of the geofluid

c_g = specific heat capacity for geofluid

$\dot{E}_L$ = exergy loss rate in kW

$\dot{E}_D$ = exergy destruction rate in kW

c_p = specific heat capacity for ipentane

$\dot{m}_a$ = mass flow rate of the isopentane

W = work output in kW

$\eta_{is,dry}$ = is dry turbine efficiency

h = enthalpy in kJ/kg

ΔP = pressure drop(Pa)

η = efficiency

v_{cl} = volume flow rate through the fan

S = size of an equipment

$\dot{C}_{total}$ = the total plant(cycle)cost in $/s

$\dot{W}_{net}$ = the cycle's net work in kW

c_e = cost of a unit of electricity in $/kWh

C = cost of an equipment

$\propto$ = scaling factor

PC = purchasing cost

Q = flow rate in SCFM

N = annual plant operating hours

CRF = capital recovery factor

i_{eff} = annual discount rate

r_n = nominal escalation rate

CI = Capial Invesment

TGDC = Tanzania Geohermal Development Company

Subscripts

is = isentropic

eff = efficiency

HPT = High Pressure Turbine

LPT = Low Pressure Turbine

g = generator

P = pump

c = critical point

ST = standard conditions

OM = Operation and Maintenance

pw = producion well

o = exiting cost stream

i = entering cost stream

t = turbine

1 BACKGROUND

1.1 Introduction

The climate challenge has been a major issue in recent decades. Emissions of greenhouse gases have led to a general rise in temperature around the globe. Major contributions of these greenhouse gases have been from polluting energy sources such as fossil fuels. These energy sources are also getting depleted over time. Therefore, green sources such as geothermal energy must replace fossil fuels.

The climate and energy crisis discussed above has necessitated different countries to make a strategic target to try eliminating polluting energy sources from their energy mix. There have been challenges in adapting renewable energy sources in recent decades mainly due to high upfront risk and high total cost of implementation of these projects relative to non-renewable ones.

Significant research and development have been dedicated to finding ways to make the levelized cost of different renewable technologies cost competitive to the non-renewable ones. This thesis work is aimed at contributing to this course by looking at ways to minimize the initial exploration investment costs in geothermal fields using slim wells. The focus will be Ngozi a strategic geothermal site in Tanzania. Ngozi geothermal prospect is the top ranked field in Tanzania for the development of geothermal power development. The plan is to generate up to 200 MW by 2025. During the first phase up to 30 MW are expected to be generated. Besides production of power, brine is also planned to be utilized for commercial direct use projects.

The project is at exploration drilling phase where 3 slim holes are expected to be drilled up to a depth of approximately 1,500 m to test both the existence and size of the reservoir. With the objective of using a light and mobile drilling equipment as possible. The wells are designed to be vertical, and they will be drilled using the rotary drilling technique. The objective is to minimize exploration costs by using a small drilling rig; most probably track mounted and a reasonably small well design that will enable flow testing.

There are numerous geothermal sites around the world where full size wells have been used in geothermal explorations, for example Karisimbi in Rwanda. This has resulted to a very high initial investment cost. On average, a full-size well costs between 4 and 6 million USD to drill to total depth [1]. Other costs involve infrastructure costs, drilling pads and access roads. These factors form a significant cost component when a full-size rig is used in the exploration phase. A key issue here is that these costs are sunk in without confirmation of the presence of the resource and whether it can be harnessed profitably.

Besides the risk involved in starting a geothermal project in a green field, high initial capital required is one of the causes of slow industry growth over the decades. Moreover, according to different literatures, it takes 6 to 10 years to develop a green field to power plant stage[2].This is a long time in terms of investment since most projects will probably use loans.

The present work looks at the possibility of producing from slim wells. Economic comparison is made if large or full-size wells were used instead of slim wells in exploration studies. The work shall involve taking into consideration the thermodynamic parameters obtained from the

field exploration studies and the cost required for power plant equipment purchase, installation, and maintenance.

1.1.1 Renewables in the current COVID environment

Covid has played a part in restricting the fast development in renewables especially geothermal energy. Companies have been forced to reduce their working capacities, limiting movements of workers since many areas in the world have restricted movement. Geothermal exploration requires a lot of movements for data collection for example. In Ngozi project, covid prevented the importation of the drilling rig and timely procurement of drilling equipment.

Despite the challenges of COVID-19, renewables were set to grow by 4% reaching 200 GW in 2020. The growth is expected to continue in 2021 where renewables will reach around 218 GW. The expected share of renewables in the global generation mix is expected to expand to a record 33% thus overtaking coal as the largest source of electricity generation by 2025. [3].

Renewable electricity demand experience growth despite the harsh COVID-19 environment experience in this year. This generally shows the resilience of the renewables compared to other sources of energy. This is mainly due to two issues, first renewables operate with long term contracts hence they are less affected by fluctuations in demand or prices and secondly, renewables are usually dispatched first into the grid (they are usually prioritized) owing to supportive government policies[3]. This is a very attractive scenario from an investor´s perspective.

Looking at the long-term future, the share of renewable energy is almost guaranteed to increase due to commitment of different nations to net zero emission. The intergovernmental Panel on Climate Change (IPCC) agreed to cut off emission by half in 2030 and reaching net zero by 2050 [4]. China has committed to net zero goal by 2060 while South Korea and Japan have set the same target before 2050 [3].

1.2 Risk factor in geothermal investment

Figure 1 below shows risks involved in different phases of geothermal development from a project idea to the production stage. It indicates that when the project starts; during pre-survey, geoscientific exploration and exploration drilling, the risk involved is extremely high. It is important to note that the bankability of the project is very low at this stage. It can also be seen that once test drilling starts; costs start to rise exponentially. This contributes to huge early investment cost when using full size wells in test drilling.

There are many risks in geothermal development such as delayed completion, price risks, offtake risk and operational risk. However, exploration drilling is the riskiest part in geothermal project implementation. This phase requires huge expenditure accounting up to 15% of the total capital investment[5]. Slim wells can be used to lower the risk and costs in test drilling as much lower costs are spent in confirming the resource, at a shorter time and offering the same information during well testing as the full-size wells. The fact that successful slim wells can be used to produce electric energy will offer extra cost reduction to the project and improve its bankability.
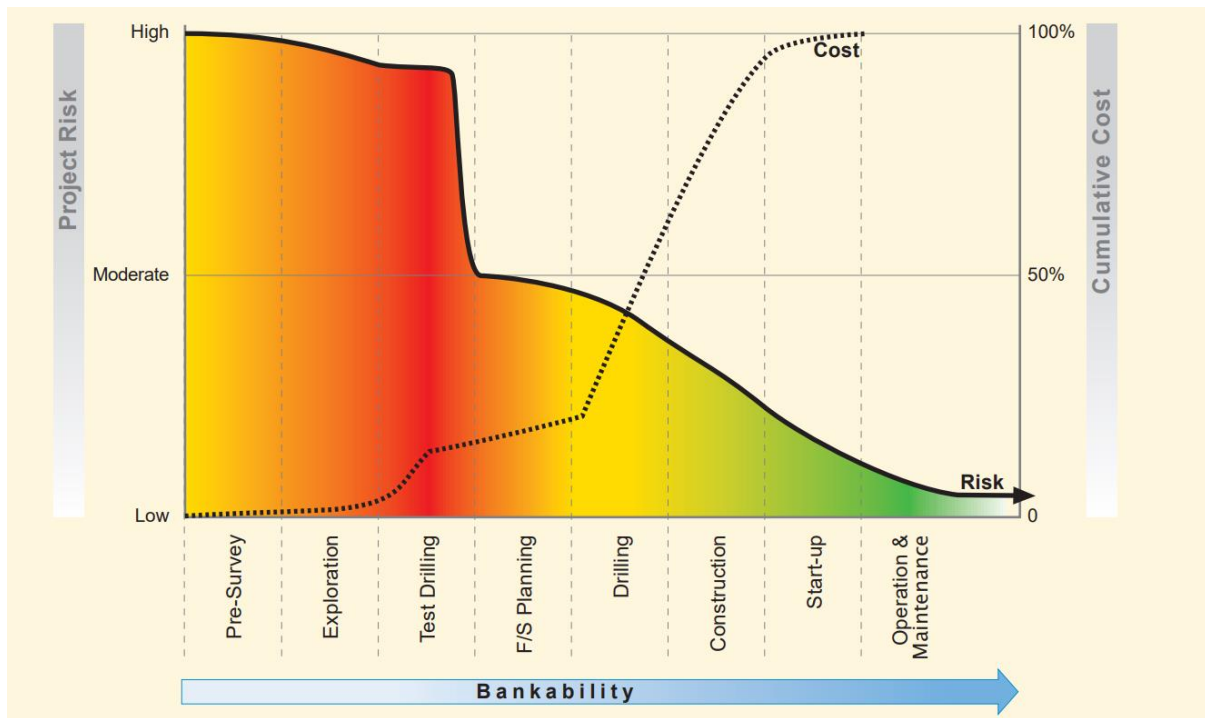
FIGURE 1: Risk in different phases of geothermal development[5]

1.3   Electricity sector in Tanzania

The installed electric capacity in Tanzania is presently over 1,602 MW, derived from hydro (31%), gas (48%) and other fossil-based production fuels (18%). The rest is solar power and biomass[6]. Due to dependence on hydropower as the baseload, the country's electricity supply has been very vulnerable to droughts. Moreover, sedimentation in the reservoirs has caused huge challenges in hydroelectric production. These challenges have resulted to power shortages in recent decades. Also, the huge dependence on fossil fuels contributes to both pollution and high prices of power in the country. The above issues have derailed the country's transition from agriculturally based economy to industrial based economy.

Tanzania has electricity consumption per capita of 133kWh per year. This is way below the world average which is 2500 kWh per year. It is important to also note that the annual electricity demand rate grows at a rate of 10% to 15%[7]. In consideration of the above, the Government of Tanzania intends to diversify the energy generation mix, focusing on an increase of the proportion of renewable energy generation, including geothermal. Diversifying the energy mix should increase energy reliability and energy efficiency. As can be seen in figure 2 below, the major consumers of electricity for the last decade have been households. Due to the requirements to promote economic growth through industrialization, which is the current economic transformation strategy in Tanzania, it is very important to ensure reliable supply of electricity through renewable sources.
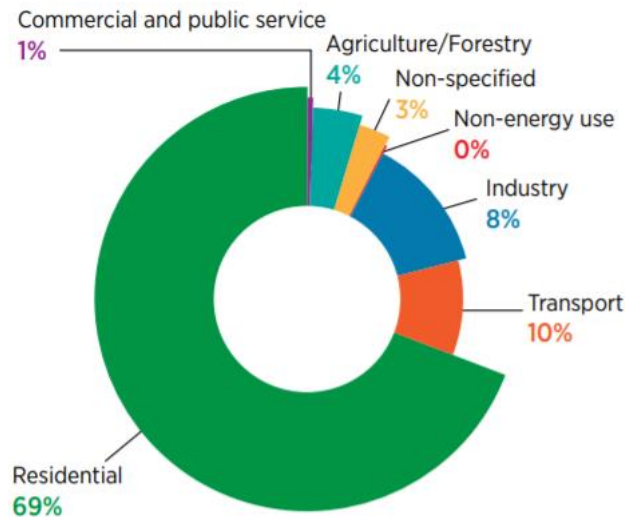
FIGURE 2: Electricity usage in Tanzania[8]

1.4   Geothermal development in Tanzania

There have been activities related to geothermal development in Tanzania as far back as 1976 when reconnaissance studies were conducted. Fifty (50) hot springs were sampled in different regions of the country. Currently the focus is on four strategic sites: Mbaka-Kyejo, Ngozi, Luhoi and Songwe. Figure 3 below shows the timeline of geothermal activities in Tanzania.
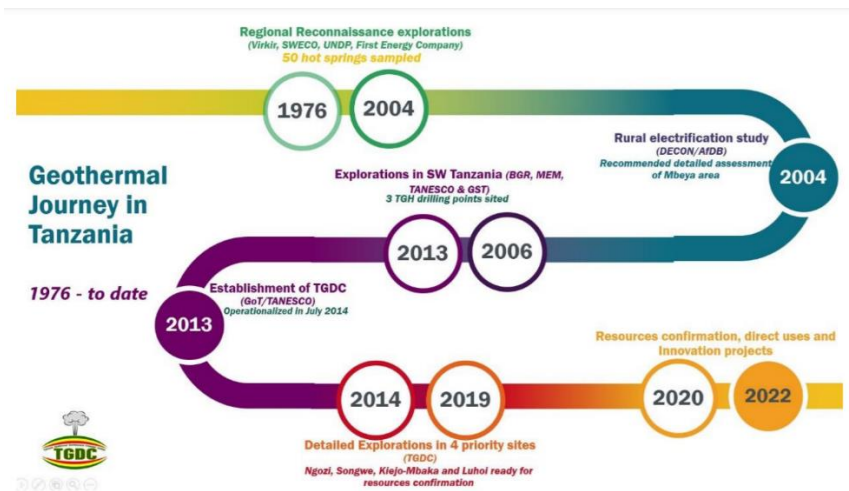
FIGURE 3: History of activities related to geothermal energy development in Tanzania[9]

To accelerate the development of geothermal energy resources in Tanzania, the government established Tanzania Geothermal Development Company Limited (TGDC) the sole company in Tanzania responsible to spearhead the development of geothermal energy. The company has undertaken several projects, but the main project is the development of the Ngozi geothermal field, which is in test drilling phase of three slim wells up to a vertical depth of 1500m.

It is common for most geothermal sites to be associated with certain rift system. Tanzania has both the western and eastern (East African Rift System (EARS)) rift system crossing the country. Tanzania has an estimated geothermal potential of over 5000 MW[9]. This huge

potential has not been exploited until recently. The estimated potential is broken down site wise in table 1 below.

TABLE 1: Estimated geothermal potential in Tanzania[9].

S/N	GEOTHERMAL POTENTIAL	ESTIMATED CAPACITY
1	**Southwest Volcanic province – Mbeya** (Ngozi, Songwe, Mbaka-Kiejo)	1,000MW
2	**Nyasa – Mbeya - Rukwa zone**	800MW
3	**Central Zone – Dodoma, Singida & Shinyanga.**	500MW
4	**Morogoro region** (Kisaki)	600MW
5	**Coast region** (Luhoi, Utete in Rufiji)	600MW
6	**Lake Zone (Mara, Shinyanga, Kagera)** (Maji Moto, Ibadakuli, Mtagata)	500MW
7	**Northern Volcanic region (Arusha – Kilimanjaro)** (Natron, Manyara, Eyasi, Ngorongoro)	>1,000MW
	TOTAL ESTIMATED POTENTIAL	>5,000MW

1.5 Ngozi geothermal field

Tanzania´s geothermal resources are comprised of 4 geological settings. These are the south-western and northern volcanic province, intra-cratonic geothermal system, coastal basin, and the western rift system[9] as shown in figure 4 below. Ngozi is in the South of Tanzania a region called Mbeya. The site is an active volcano that is part of south-western volcanic province and is situated in the triple junction of East African Rift System (EARS)
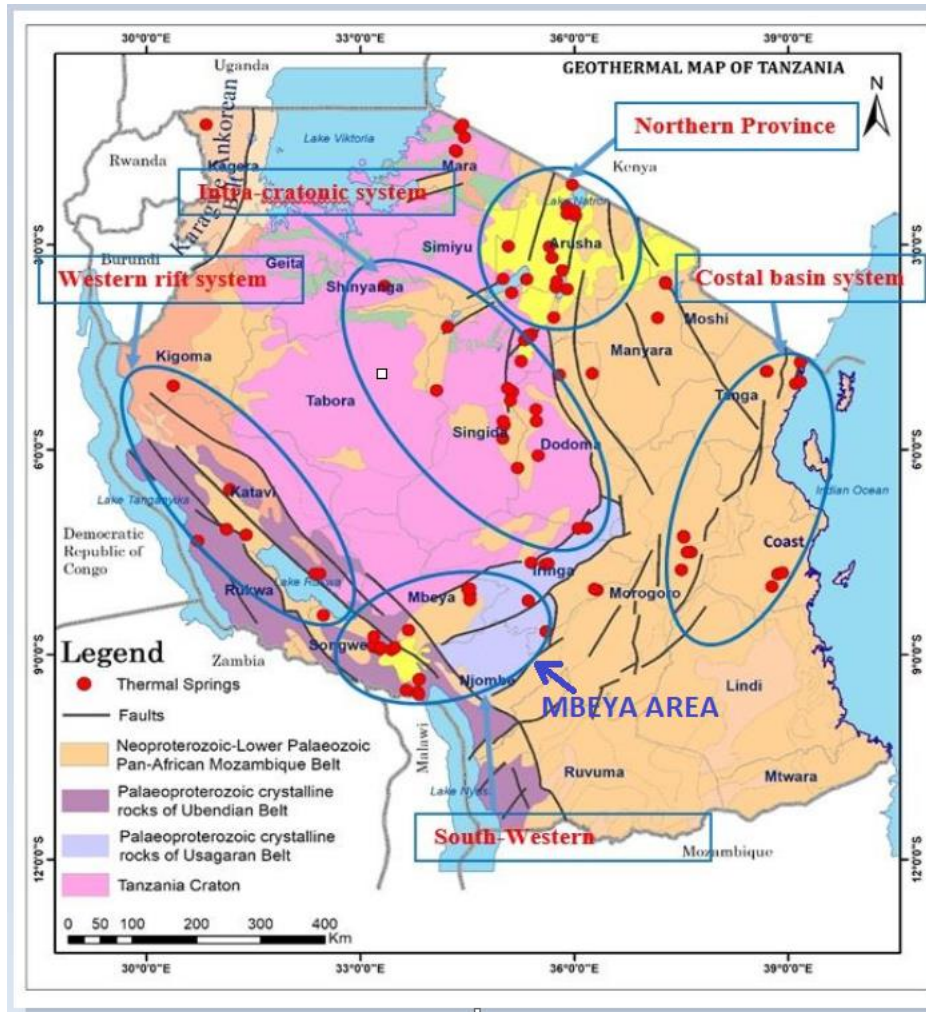
FIGURE 4: Map showing the location of Ngozi[9]

Studies about the Ngozi reservoir have indicated that the reservoir is accommodated either in the most recent intrusive neck of the Ngozi volcano or in old volcanic rocks or in intrusive rocks related to deep dykes and old magma chambers. The cap rock consists of volcanic rocks that have been hydrothermally altered. The lateral extent of the reservoir is constrained, amounting to 12 km^2 for P10, 2.9 km^2 for P50 and 0.6 km^2 for P90[10].

Since no wells have yet been drilled in Ngozi, there is limited information about expected pressure and temperature conditions that will be encountered by planned slim wells in Ngozi. Geoscientific studies estimate the reservoir temperature to be around 232±13 ° C[10].

There is an existing power line near Ngozi project. This will facilitate the transport of electricity when full production commences. Moreover, Ngozi prospect is 18 km from Mwakibete substation[11] which has 220 kV electricity transmission line connecting to the national grid.

1.6 Introduction to slim wells

There are several definitions that describe slim wells from literature. Slim wells are defined by the society of petroleum engineers as wells with casing less than 7-inch in diameter for 90% of the well's depth[12]. Also, according Thorhallsson and Gunnsteinsson [13], slim wells are

defined as wellbores with final diameter of less than 6 inch. This is the most used slim well definition in the geothermal industry, and this literature will apply it.

Slim wells have been used in the past. However due to limited technological advancement, they did not reach very deep and therefore their cost savings were not economically justifiable which limited their acceptance[13]. Currently slim well rigs are designed to go as deep as 2.5 km. they can drill using tricone bits or coring drilling bits. Their hook load ranges between 20 to 100 tonnes. The smaller the rigs the better because of the mobility advantage since most of the exploration sites are usually remote, as well as reduced environmental footprint from the drilling.

As mentioned above, given good reservoir permeability, slim wells can flow. This will enable the collection of crucial well testing information and even analyse the possibility of producing from them. Mackenzie et al [14] conducted a study for the slim wells drilled around the world. The study showed that 62% of slim wells investigated were flowing after drilling (figure 5). Also, 73% of the wells, successfully intersected the reservoir meaning crucial information about the reservoir could be collected from the slim wells.
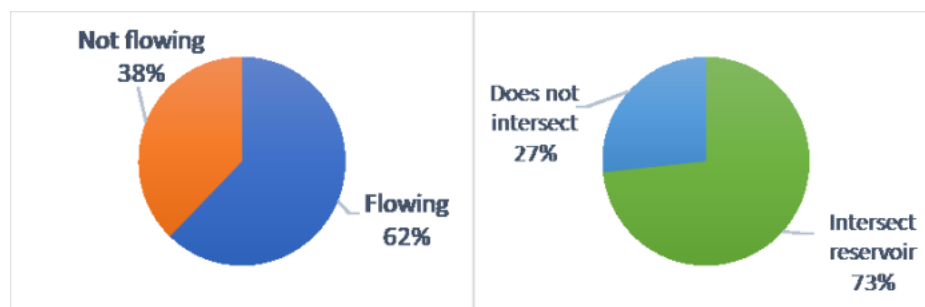
FIGURE 5: world-wide slim well drilling data[14]

For liquid dominated reservoirs the injectivity index and productivity index are approximately the same irrespective of the well diameter[15]. This is one of the reasons slim wells can be very usefully in determining productivity index for full size wells.

1.6.1   Slim holes over full size wells

According to Finger et al. (1999) drilling slim wells instead of full-size wells during exploration produces cost savings of up to 60%[16]. This is also supported by the study by McKenzie et al.;(2017) the cost of drilling a 1500m slim is between USD 1.3 m and USD 1.8 m depending on different factors such as location of the rig [17]. This cost compared to the cost of drilling a full size well (between 4 and 6 million USD), enables cost saving of an equivalent amount. Drilling is cheaper for slim wells than conventional production wells because the rigs are smaller and casing, cementing, crews and drilling fluid requirements are all reduced[13].

In addition, the success rate in geothermal exploration drilling is 25%-40%[18]. This means, on average, for every three wells drilled in a geothermal field one will be a dry well. Thus, the cost of failure is quite high. Slim wells can significantly lower the cost of failure and help the developer to avoid huge debts.

Since most exploration work takes place in remote areas, huge investment is required to establish proper infrastructure before drilling starts. However, at this stage no resource has been

confirmed. Thus, it is vital to minimize construction works as much as feasible; possibly by using a truck mounted drilling rig for slim hole drilling.

The environmental footprint due to slim well exploration drilling is much smaller compared to full size well drilling. According to Nielson et al. (2017), slim wells produce much less environmental disturbance compared to full size wells[15]. Drilling has come under scrutiny and been criticized in recent years due to its environmental impact. Apart from minimizing drilling costs, the use of slim wells over full size wells would enable environmental permits to be obtained easily due to less environmental footprint and less reclamation work after drilling activities.

The discharge rate of the wells increases as the diameter of the well increases. Thus, a full size well would most likely produce more fluids compared to slim well in the same geological setting. Also, there are other factors such as heat loss and frictional pressure that are affected by the diameter of the well. The smaller the diameter of the well the higher the heat loss and frictional pressure[20].

Moreover, there are some key drilling challenges that are typical in drilling slim wells. These include drilling fluid hydraulics, tool joint failures and drilling string failures[21]. These challenges are caused by smaller clearances between the drill string and the well bore in slim wells compared to those of full size well drilling. It is important, therefore, to use an experienced slim well contractor. This will enable the developer to use less time in drilling as the contractor has the required experience to deal with the challenges.

Lastly, less drilling fluids are normally used in slim well drilling compared to full size well drilling. Slim well drilling typically use 0.8 litres per second to 1.3 litres per second of drilling fluid compared to over 25 litres per second of drilling fluids used to drill full size wells [22]. Even less volumes of drilling fluids may be used when drilling slim wells with coring rigs. Drilling fluids can be a huge challenge especially at drilling sites where there is no water infrastructure set up and/or water is scarce. The developer can just use water tanks to bring drilling water to the drilling site for slim well drilling. However, if full size wells are being drilled at this stage, full scale investment in water infrastructure must be carried out.

1.6.2   Nature of slim well costs

Cost distribution in a geothermal field is represented by figure 6 below. The major cost drivers are drilling and electromechanical equipment purchase. Since this study focuses on drilling, it is important to note that drilling forms 30 to 40 percent of the total geothermal project cost. This means minimizing drilling cost will eventually minimize the cost of the project. The other most significant cost component is the electromechanical equipment costs such as the turbine. A MATLAB model is developed in the present work, which is utilized to optimize both drilling cost and electromechanical costs for the Ngozi project.
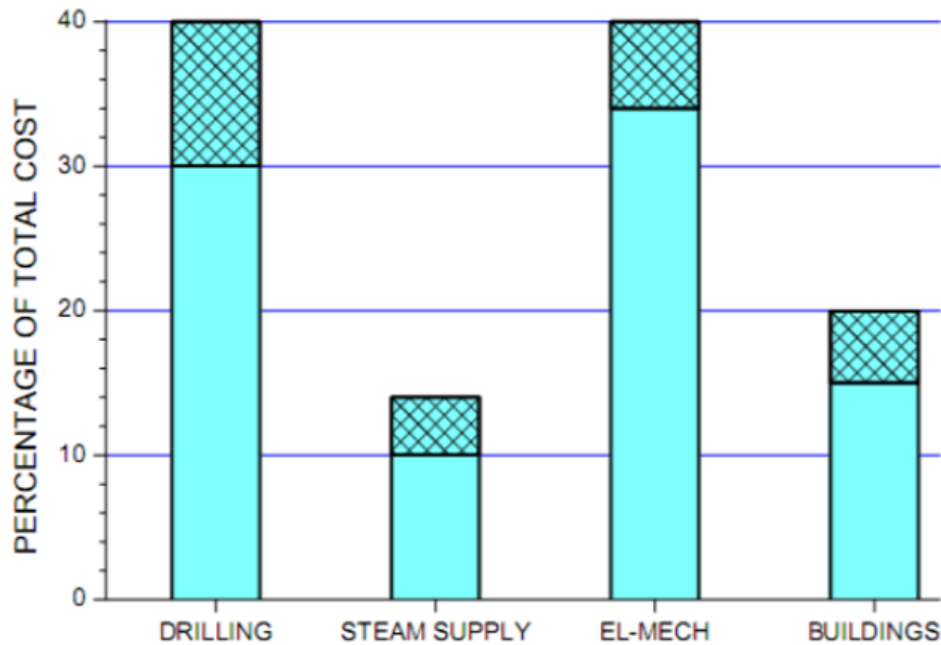
FIGURE 6: Geothermal project cost breakdown[23]

Furthermore, the rig operation costs are a dominating cost factor in slim drilling. Usually drilling rigs are hired and operated by a third-party contractor. It is important to have clear contract with the contactor. Drilling contracts include day rate, turnkey, and meter rate contracts. TGDC is expecting to hire a contractor to operate on day rate terms. Daily operating rates include the daily rig rate which is the rental charges for the rig with crew and associated equipment.

To take advantage of the comparatively short drilling time for slim wells compared to full size wells and hence reduced drilling costs, it is important to solve problems that arise during drilling of slim wells fast. This can be done by having clear chain of command and clear decision-making protocol.

1.6.3 Slim hole design in Ngozi

Slim wells are usually designed using different industrial standards; most importantly the African Union Code of Practice for Geothermal Drilling. It is important to have a proper design so that the wells can be flow-tested. Assuming that there will be adequate permeability in Ngozi, the slim holes are expected to "self-flow".

However, the Ngozi slim well design includes the possibility of using a down hole pump to initiate the flow of the well in case the well does not flow by itself. Coring can also be used in slim well drilling. This enables core samples to be collected. Coring is usually done in the last drilling section to obtain crucial information about the reservoir.

Ngozi slim well design was done in the literature by Lubuva,2018[24]. The design well head pressure is 74.37 bar, and the temperature is 290 degrees centigrade. The temperature value is different from the reservoir temperature of around 232±13 degree Centigrade estimated by Alexander et al., [9] because design considerations assume a "worst-case scenario" for the pressure and temperature conditions with respect to well control since no wells have been drilled in the area.

1.7   Slim and full size well data from Japan

Due to the lack of availability of well testing data in Ngozi project, a geothermal case study from Japan was used as a basis to run the proposed power cycles (discussed below). The study was carried out by Pritchett J. W.[25]. It contains well testing data for both slim well (less than 6'' or less than 15 cm) and full-size wells drilled in Japan.

The field is liquid dominated and low enthalpy as shown by data in table 2 below, with wells being drilled to 1500 m. The reservoir temperature and pressure are 250 degrees centigrade and 80 bars, respectively. These conditions are like the predicted conditions at the Ngozi geothermal field, which is why the results from this study were selected for use as input data.

It would make little sense to say that slim wells are cheap. Since the term cheap is subjective. Comparing slim well cost and full size well cost makes a more compelling case. However very few geothermal fields have well testing data for both slim well and full size well available for the analysis. That is another attractive feature of the data for the geothermal field in Japan. Another field that could provide comparable data is steamboat USA.

The case will be used to simulate different final the cost of power and other performance parameters for different final diameters of the well. The comparison between the performance parameters of the slim wells and full-size wells will be compared using data from this case. Results of the simulation are expected to show how the choice of a certain final well diameter will affect key parameters such as the net-work output and the price of a unit of power and efficiency of the power cycles.
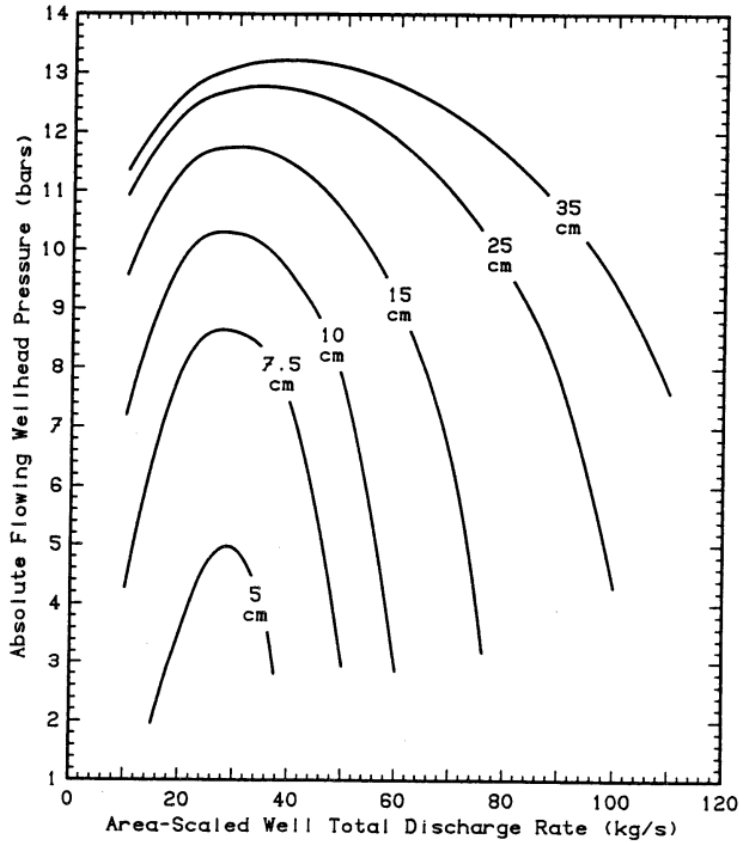
FIGURE 8: Pressure curves as a function of mass flow rate for different well diameters [25]

Selected pressure and temperature values are picked from the characteristic curve of each diameter of the well. These data were used in the different proposed power cycles (single flash cycle, binary cycle, and double flash cycle) that are discussed below and the results were analysed. Table 2 shows selected points from each well characteristic curve (different wellbore diameters) in figure 8 above.

TABLE 2: Selected data from Pritchett J. W.

Wellbore diameter (cm)	Discharge rate (kg/s)	Pressure (bars)	Enthalpy (kJ/kg)
SLIM WELL DATA			
5	30	4.94	743.9
7.5	32	8.58	912.28
10	34	10.19	982.5
15	40	11.58	1037.2
FULL SIZE WELL DATA			
25	47.77	12.7	1060.8
35	54	13.18	1066.7

2   THERMODYNAMIC EVALUATION

The laws of thermodynamics directs the movement of thermal energy between the system and the surrounding and the relationship between heat, work and properties of the system at equilibrium[26]. A typical thermodynamic system such as a geothermal power plant, uses heat input to produce work. The laws of thermodynamics limit how much of the heat can be converted to work, and in addition, there will always be losses during the process. The thermal efficiency of a thermodynamic system can be defined as the ratio of net-work to energy input as shown in the equation below:

$$\eta_{th} = \frac{net\ work}{heat\ input} \tag{1}$$

In designing an optimized power cycle system, the first step is to come up with a workable design. To obtain this, different power cycles which can be used for the production electricity are, in the present work, applied to the Ngozi geothermal resource case study. The cycles are single flash power cycle, double flash, and binary power cycles. Input parameters include pressure, enthalpy, and mass flow rate that are provided in table 2 above for different wellbore diameters.

2.1   The proposed power cycles.

2.1.1   Single flash cycle

Single flash steam power plants are very common in liquid dominated fields. These type of cycles account for around 29% of geothermal power plants around the world[27].

Cycle description:

As can be seen in figure 9 below, the cycle starts with geothermal fluid flowing from the well; stream 1. The fluid passes through the throttle valve where pressure is regulated to get the required separation pressure. From the separator, stream 3 which is a saturated vapour stream flows into the turbine for power generation while liquid geothermal fluid; stream 4 leaves the separator as condensate(brine) that is to be reinjected to the reinjection well.

On the other hand, exhaust fluid from the turbine (stream 5) goes into the condenser where it is condensed into saturated liquid (brine), which flows back to the reservoir through the reinjection well; stream 6.
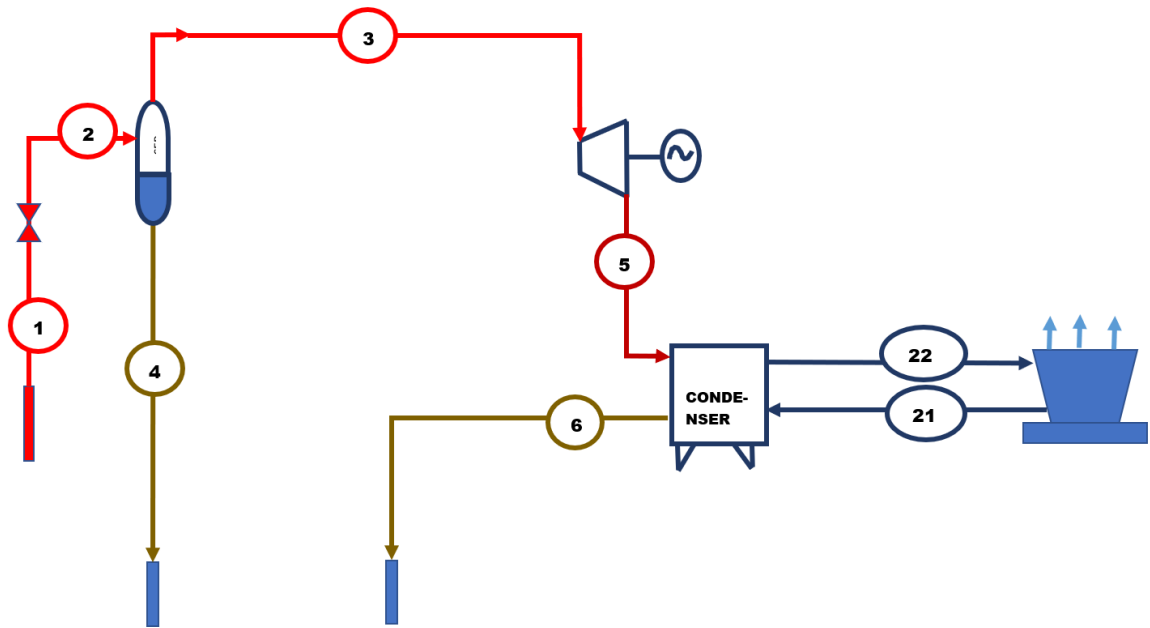
FIGURE 9: Single flash power cycle

2.1.2 Double flash cycle

This cycle uses two separators (high pressure separator (HPS) and low-pressure separator (LPS)) and two turbines; one a high-pressure turbine (HPT) and a low-pressure turbine (LPT)) as shown in figure 10 below. The introduction of an additional turbine in double flash is supposed to increase the net power output, compared to single flash turbine. The net increase is usually in a range of 15%-25%[27]. However, the cost implication associated with addition of an extra turbine and separator must be weighed up against the benefit of adding extra megawatts in the grid, that are normally greater for higher enthalpy geothermal fluids than are available in this study. A thermo-economic analysis is preformed to determine the cost-benefit analysis of such effect.

Cycle description:

Geothermal fluid flowing from production well; stream 1 passes through the throttle valve; stream 2 where pressure is regulated to get the required separation pressure. From the High-pressure separator (HPS), stream 3 which is a saturated vapour stream flows into the high-pressure turbine (HPT) for power generation while liquid geothermal fluid; stream 4 leaves the separator and flows through another throttle valve to regulate pressure again before the fluid enters Low pressure separator (LPS).

Stream 7, which is saturated vapour, leaves the LPS and mixes with the exhaust steam from HPT; stream 5. The mixture then enters the LPT to produce power. Exhaust fluid from the low-pressure turbine; stream 10 goes into the condenser where it is condensed into saturated liquid; stream 11. The condensate from the low-pressure separator; stream 8 and stream 11 both go into reinjection well as waste fluid (brine).
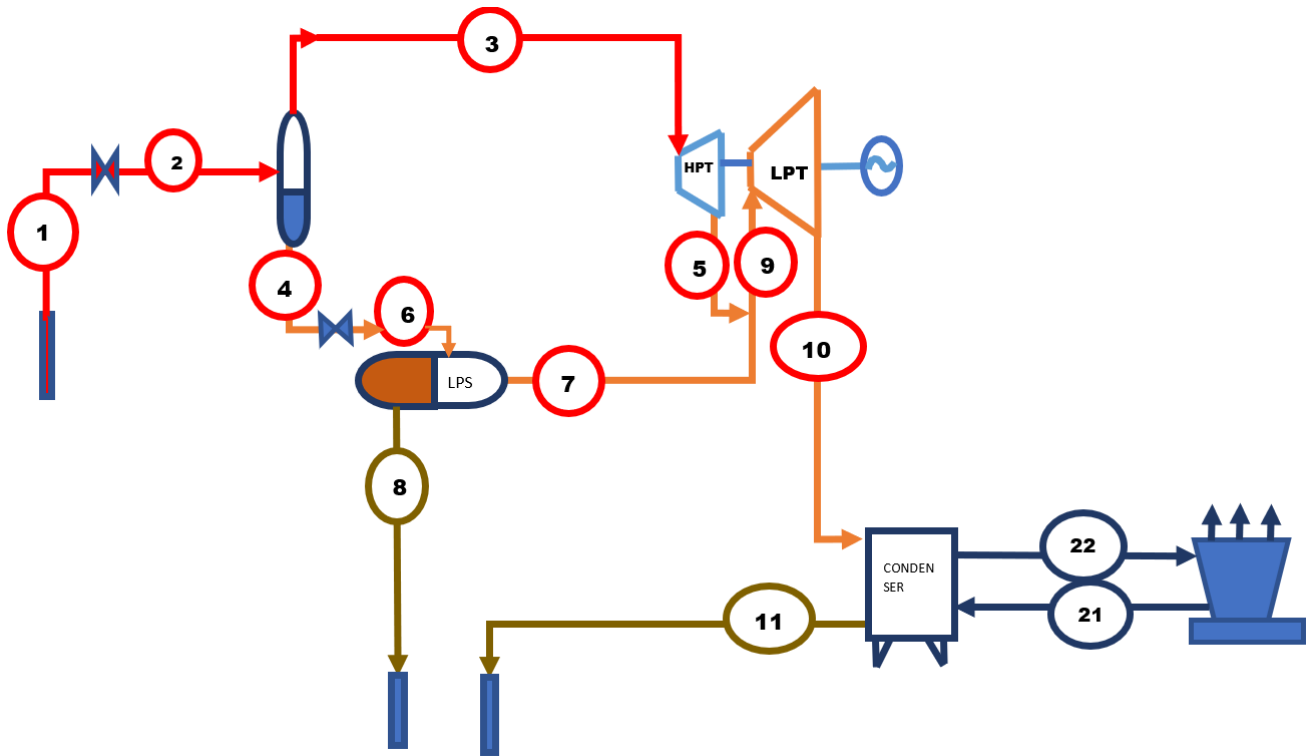
FIGURE 10: Double flash power cycle

2.1.3 Binary cycle

Binary geothermal power plants are used to produce power from medium temperature and low temperature resource through evaporation of a secondary organic working fluid. Low temperature geothermal resource is the one that has a maximum temperature of 150 degrees Celsius at 1000m while medium temperature resource has a temperature range between 150 degrees Celsius and 200 degrees Celsius at 1 km depth [28].

Binary plants are the most extensively used units in geothermal industry with the average power production of 3 MW/unit[27]. To decrease energy waste and improve efficiency in production, these units are sometimes coupled to single flash plants, as bottoming cycles, to gain extra MWs from brine before reinjection. With the continued technological development binary power plants could play a key role in the development of geothermal industry since most of the geothermal resources are characterized as low temperature resources where binary power cycles are most practically applicable. Binary technology has been used to produce electricity from resources with temperatures as low as 57 degrees centigrade in Alaska, USA[29].

 Organic fluids used in geothermal binary cycles can be characterised as dry fluid, that include isopentane, benzene and pentane; and wetting fluids such as R134a and water[30]. The dry fluid isopentane will be used in this study due to less chance of damaging the turbine blades since it is dry. Other reasons for selecting isopentane is its environmental friendliness.

Cycle description:

Figure 11 below shows the binary circle configuration. Geothermal fluid flows to the evaporator from the production well; stream 1, then through the preheater and finally to reinjection well (stream 3). In the process, heat is transferred from the geothermal fluid to the working organic fluid of the binary cycle.

The vaporized working fluid from evaporator; stream 10, flows to the turbine to produce power. Exhaust working fluid from the turbine; stream 12 goes into the condenser where it is condensed into saturated liquid. Then its pressure is raised when it goes through the pump to produce high pressure liquid; stream 14. The fluid goes through preheater and then evaporator where vaporized organic fluid is produced again, and the cycle repeats.
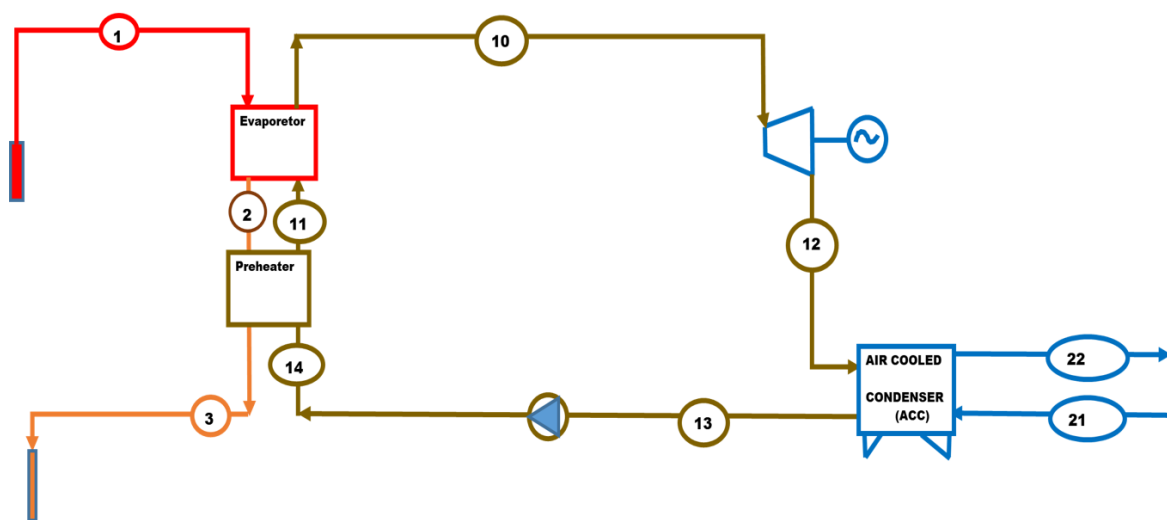
FIGURE 11: Binary power cycle

The binary power plant configuration considered here is the basic design. To improve thermal efficiency and utilization efficiency more complex designs can be investigated, such as double pressure binary cycle, dual fluid binary cycle and Kalina binary cycles.

2.2   Key assumed parameters.

The ambient conditions including temperature and pressure depend on the location of the project. The highest temperature over 10-year period at Mbeya Tanzania was 29 degrees centigrade [31] as represented in figure 12 below. Thus, the ambient temperature used in this thesis will be 30 degrees centigrade, ambient pressure was taken to be 1 bar. These values are very important because they can affect the amount of power that the plant produces.
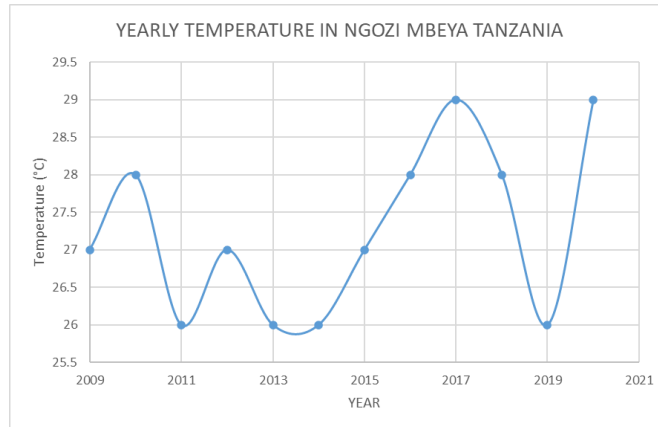
FIGURE 12: Annual maximum temperature values in Mbeya Tanzania[31]

Uhorakeye, T. [32] and Salas, J.R.E [33] refer to the overall heat transfer coefficient between geothermal fluid (brine) and isopentane as 1200 W/m^2. K This will be used for the preheater and evaporator.

Other parameters used in this paper include:

- Geothermal power plants usually have a high-capacity factor. For this thesis, the plant capacity factor of 90% will be used in calculation. Therefore, the assumed plant operation hours per year is 7884.
- Operation and maintenance cost 20% of the purchased equipment cost for each respective equipment.
- The system economic life is 20 years.
- The geothermal fluid properties will be assumed to be equivalent to pure water properties in state properties calculations.
- According to the organization for economic cooperation and development (OECD), Interest rate for projects whose life is more than 18 years is usually around 3.54%. Thus, for this thesis 4% interest rate will be used[34].

2.3 Scaling

One of the most challenging issue in utilizing the geothermal fluid has been the chemistry of the fluid. For a given geothermal field, its fluid chemistry may cause deposition of minerals in different components of the power plant and pipes. This phenomenon is called scaling. This has considerable implications for operational cost of the project since it may increase the frequency at which maintenance works have to be carried out. This challenge often includes shutting down the operations of the power plant.

There are different types of scaling in geothermal environments, however calcite scaling ($CaCO_3$) and silica scaling (SiO_2) are the most common [35]. Solubility of silica increases as the temperature of the resource increases (keeping other factor constant such as pH). This means in a high temperature resource that silica is expected to be more of a problem during production than in a low to medium temperature resource. Moreover, double flash power plants face a higher risk of silica precipitation due to higher temperatures of the geothermal fluid and the fact that the second separator lowers the temperature of the fluid further compared to single flash plants.

If scaling occurs in the plant equipment such as pipes, it will lead to reduced performance efficiency of the equipment, whereas it may also occur in the reinjection well or reservoir resulting in lowering of permeability[27].With reference to figure 13 below, scaling depends on the concentration of silica in the geothermal fluid as well as the temperature of the fluid. Right now, there is no data on the concentration of silica in the Ngozi geothermal project since slim hole have not been drilled yet. According to Gunnlaugsson et al.,[35]; to avoid scaling, temperature of the geothermal fluid throughout the cycle should be kept above the solubility curve of amorphous silica as shown in figure 13 below.

Another option to mitigate scaling is the use of binary plants; since in the binary power plant there is no flashing of the geothermal fluid[27]. Also, geothermal fluid only encounters the secondary fluid in the heat exchanger, other key plant equipment such as the turbine, pump and the condenser have no contact with the geofluid unlike other types of power cycles. This reduces the risk for scaling in the plant equipment. However, cooling of the geothermal fluid still occurs hence the precipitation risk still exists in the well and reservoir. Proper design will mitigate the later risk.
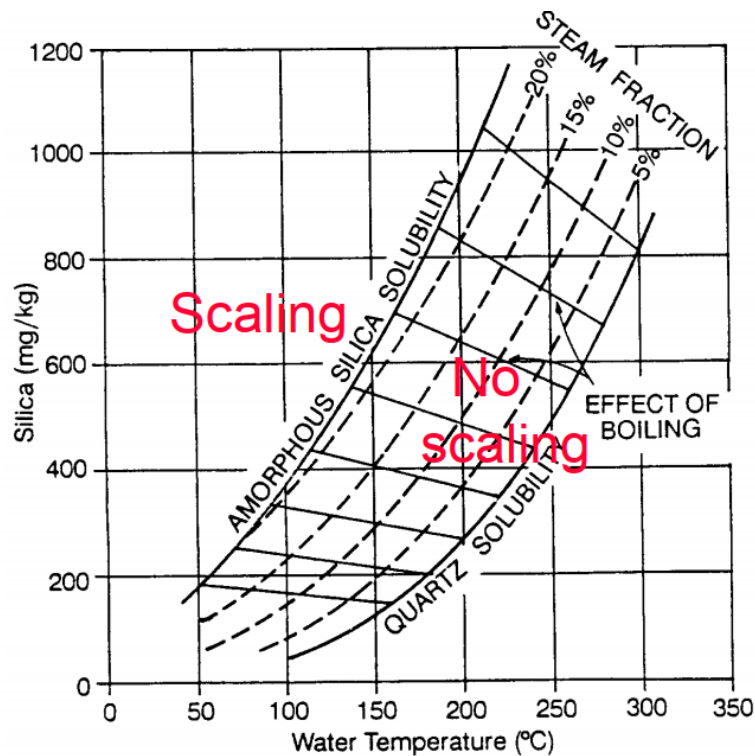
FIGURE 13: Solubility of difference forms of silica in water[35]

There are several practical ways used in geothermal industry to deal with scaling issue once it has already occurred. These include using different scaling inhibitors, reaming the well to remove depositions, and changing well head pressure to alter the level at which scaling occurs in the well. It can be observed from figure 14 below, that increasing well head pressure moves the flashing point and hence scaling towards shallower depth. This will enable the well to continue producing while planning for further mitigation measures such as rig mobilization to ream the well.
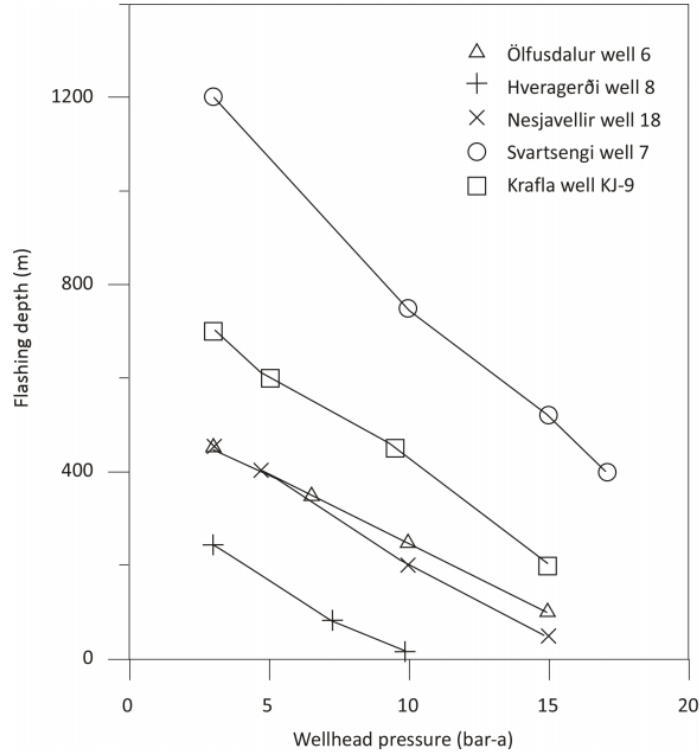
FIGURE 14: Effects of pressure change on scaling[35]

The optimization process performed in this thesis will considers the minimum temperature that will prevent precipitation of silica in power plant equipment, well and reservoir. Hot reinjection of the fluid will be carried out to avoid scaling problems.

Mokarram et al. [36] conducted a study on an organic Rankine power cycle; in which they showed that the temperature of the condensate fluid that will be reinjected should be greater than 70 degrees centigrade to avoid scaling. Since there is no data on the amount of silica concentration Ngozi, the above constraint will be used in the power cycles models as also represented by equation 2 below:

$$T_{re-injection} > 70\ degrees\ centigrade$$

(2)

2.4 Major equipment in the cycles

All the power cycles are made up of some common basic equipment. It is only the arrangement, capacity, and type of working fluid used that distinguishes between them. The cycles' major components including separator, turbine, condenser, pump, cooling tower and generator. These components and their key thermodynamic equations are discussed below:

2.4.1 Separator

The separator is an important component in the steam power cycle. It is used to produce steam from a two-phase geothermal fluid. This happens due to difference in densities between the two phases. The separation process is assumed to occur at constant pressure. The condensate is removed from the separator and returned to the reservoir through the reinjection well in the case of a single flash arrangement.

18

Separation pressure (or temperature) in both single flash and double flash should be optimized thermo-economically, so that maximum power is obtained from the cycles while minimizing the total costs. However, scaling is one of the limiting factors in the Separator pressure (or temperature) optimization. Considering figure 9 of the single flash cycle, the separation process is an isobaric process:

$$P_2 = P_3 = P_4 \tag{3}$$

Also, in the process mass is conserved,

$$\dot{m}_2 = \dot{m}_3 + \dot{m}_4 \tag{4}$$

The steam dryness fraction, x can be calculated using the equation below:

$$x = \frac{h_2 - h_4}{h_3 - h_4} \tag{5}$$

2.4.2 Heat Exchanger

The analysis of heat transfer through the heat exchanger discussed in this thesis focuses on the preheater and evaporator in the binary power plant cycle. The type of heat exchanger used in the designs in this thesis is counterflow, surface heat exchanger where the fluids do not come into contact with each other. This is advantageous especially in geothermal environment where the chemistry of the geofluid cause a lot of problems in the vital equipment of the power cycle such as the turbine.

Figure 15 below, called the temperature-heat transfer diagram is used to analyse heat transfer through the heat exchangers (preheater and evaporator) in the binary cycle. It is used to determine the pinch point. Pinch point (ΔT_P) is the minimum temperature difference between geothermal fluid and the working fluid. There is a trade off in determining the pinch point. It is normally preferred to have a pinch point of zero that means all the heat from the geothermal fluid has been transferred to the working fluid for power production. However, this will be too expensive and economically unfeasible. For a given design the pinch point is usually thermo-economically optimized.
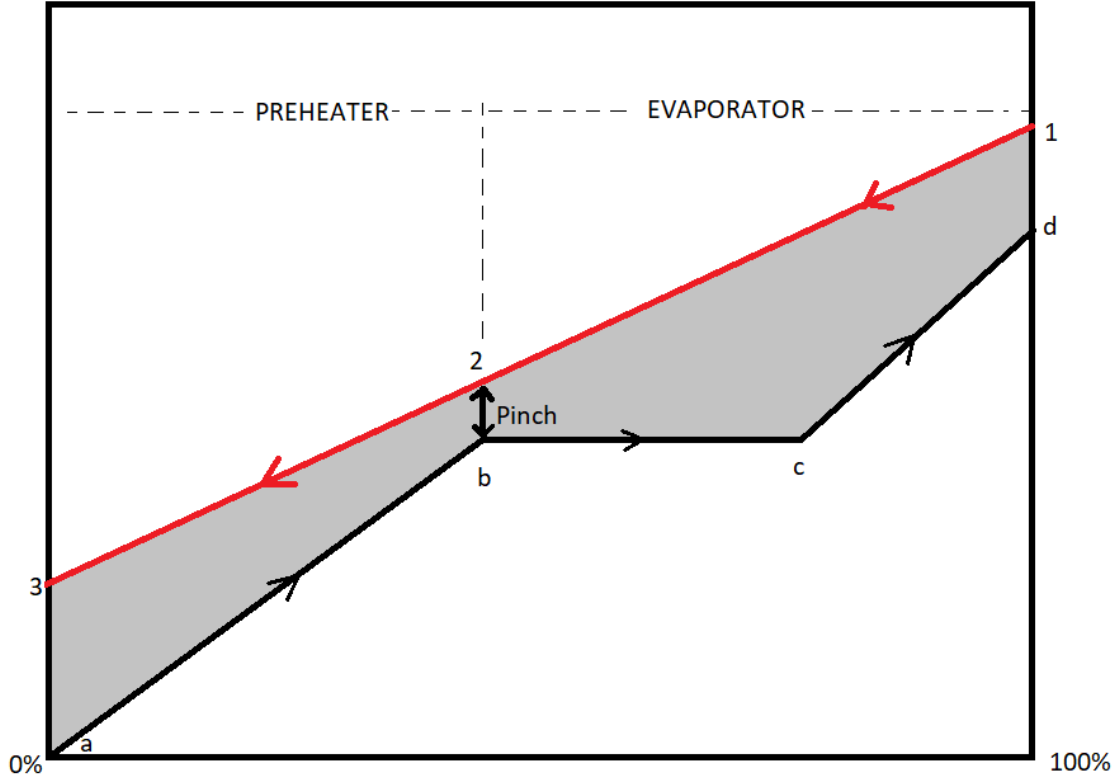
FIGURE 15: Temperature-heat transfer diagram

Heat transfer through the preheater from the geothermal fluid to working fluid (isopentane in this case) is used to raise the temperature of the working fluid to its boiling point. This is represented in step a-b in figure 14 below. The evaporator (step b-d) involves two steps, steps (b-c) where state change occurs in the working fluid at constant temperature. The fluid is saturated at this point with both gas and liquid. Then from point c, gas increasing up to point d where the working fluid became 100% vapour. Step (c-d) is the superheat.

The geothermal fluid cooling curve (1-3) and the working fluid heating curve should be designed as close as possible to maximize the use of the exergy present in brine, thus increasing utilization efficiency.

Heat transfer from brine will be equal to heat received by the working fluid according to the principle of energy conservation. Thus, heat transfer, $\dot{Q}$ was given by:

$$\dot{Q} = \dot{m}_1 * c_g * (T_1 - T_3) = \dot{m}_a * c_p * (T_d - T_a) \tag{6}$$

Also, the heat transfer area for the heat exchanger, A which is a very important parameter that affects the cost of a heat exchanger will be calculated as follows:

$$A = \frac{\dot{Q}}{U * \Delta T_{lm}} \tag{7}$$

Considering ΔT_1 as the temperature difference between the hot inlet and cold outlet as well as ΔT_2 as the temperature difference between the hot outlet and cold inlet streams, then, the log-min temperature difference, ΔT_{lm} is defined as

$$\Delta T_{lm} = \frac{\Delta T_1 - \Delta T_2}{In \left(\frac{\Delta T_1}{\Delta T_2} \right)}$$ (8)

2.4.3 Turbine

The turbine converts the energy contained in geothermal fluid into rotational mechanical energy through expansion. The pressure and temperature of the geothermal fluid drops. The turbine is a very important and expensive part of the power cycle. Considering figure 9 for the single flash cycle, the work done by the turbine is represented by the equation 9 below. Work output for the double flash is equal to the summation of work produced by high pressure and low-pressure turbine.

$$W_t = h_3 - h_5$$ (9)

The efficiency of the turbine called isentropic efficiency is an important parameter. It is usually less than or equal to 90%. Determination of an optimum efficiency is very crucial because the bigger the efficiency the more the power produced by the turbine. However, the higher the efficiency of the turbine the more expensive it is; therefore, a trade-off is inevitable. A typical efficiency used here will be 85%.

It is known that the turbine usually operates in the wet region. Thus, it is important to calculate and use wet turbine efficiency. According to Dippipo[27], a decrease in efficiency of approximately 1 percent occurs when the wetness of the fluid entering the turbine increases by 1%. Wet turbine efficiency, η is calculated using the equation below:

$$\eta_{eff.} = \eta_{is,dry} * \left(\frac{x_3 + x_5}{2} \right)$$ (10)

Where x_3 is assumed to be equal to 1(Steam entering the turbine is assumed to be completely saturated). Thus, calculating the actual exit enthalpy of the turbine h_4

$$h_5 = h_3 - \eta_{eff.} * (h_3 - h_{5is})$$ (11)

2.4.4 Condenser

The condenser is water cooled with water being pumped from the cooling tower. It is used to condense the exhaust geothermal fluid from the turbine to a saturated liquid phase so that it can be pumped to the reservoir through the reinjection well. A very important parameter here is the inlet cooling fluid temperature to the condenser which is usually optimized for a given power cycle.

2.4.5 Cooling tower

The cooling tower will use water as a cooling medium, to enable cooling of the condenser cooling water towards the wet-bulb temperature for the siter. In the Ngozi project, water is expected to be available through shallow water wells that will be drilled in the area.

The cooling range temperature will be important input in the design of the cooling tower. Considering figure 9, heat that will be removed from the condenser by the cooling tower will be given by the equation below:

$$\dot{m}_5(h_5 - h_6) = \dot{m}_{21}(h_{22} - h_{21})$$
(12)

The parasitic load due to cooling motor fan power; $\dot{W}_{motor-fan}$ of the cooling tower is given by:

$$\dot{W}_{fan} = \frac{v_{cl} * \Delta P}{\eta_{fan}}$$
(13)

$$\dot{W}_{motor-fan} = \frac{\dot{W}_{fan}}{\eta_{motor-fan}}$$
(14)

2.4.6 Generator

The generator is coupled to the turbine and converts mechanical power to electrical power. It is important for the generator to be as efficient as possible to minimize losses. The efficiency of the generator for the power cycles considered in this thesis was 98%. Design and cost engineer must agree on the thermo economically optimum generator efficiency to be used; the higher its efficiency, the more expensive it will be. The power produced by the generator is given by the equation below:

$$W_g = \eta_g * W_t$$
(15)

3   METHODOLOGY

This thesis compares three (3) steam power cycles; single flash, binary and double flash cycles for production of electricity from Ngozi slim wells. Thermodynamic and thermo-economic analysis of the cycles is applied to determine which one is the most technically and economically suitable for this project.

As discussed in section 1.8, this study makes use of full size well data and slim well data from the literature by Pritchett J. W.[25], to compare the suitability of production of electricity from these two types of wells in the exploration phase. The analysis will be done by performing exergetic analysis of the proposed power cycles.

3.1   Introduction to exergy and exergy analysis

Exergy can be defined as the maximum theoretical useful work that is available or can be attained when a system interacts with the environment to equilibrium[37].Unlike energy, exergy can be destroyed or lost. The location where the destruction or loss occurs in a system and the exact magnitude of exergy destruction or exergy loss is of crucial importance in the study of exergy. This will enable different possibilities for improvements to be analysed for the components that cause the most exergy destruction. According to Bejan et al.[37], specific exergy of a system relative to the surrounding environment is expressed as follows:

$$e = (h - h_o) - T_o(s - s_o) + \frac{1}{2}V^2 + gz + e^{ch}$$
(16)

Where, the last term on right hand side represents specific chemical exergy and specific potential exergy. The analysis done in this thesis will ignore potential, kinetic, and chemical exergy of the system. Therefore, from equation 16 above, specific exergy; e of a system relative to the surrounding environment is given as:

$$e = (h - h_o) - T_o(s - s_o)$$
(17)

Moreover, exergy rate; $\dot{E}$ of a component in the system can be expressed in terms of mass flow rate and cost per unit exergy (specific exergy) as follows:

$$\dot{E} = \dot{m} * e$$
(18)

Exergy is generally not conserved. The sum of exergy entering a system is equal to the sum of exergies leaving the system, exergy loss and exergy destruction. The quantities exergy loss and exergy destruction provide a measure of thermodynamic inefficiencies [38]. Equation 19 below shows the relationship:

$$\dot{E}_i = \dot{E}_o + \dot{E}_L + \dot{E}_D$$
(19)

We can also calculate the exegetic efficiency of a major components in a system or power cycle. The exegetic efficiency; ε_{ex} is the ratio of exergy rate of the product to the exergy rate of fuel. The product is regarded as the desired output of the system or component and fuel is regarded as the input to the system or component required to produce the product. Equation 20 below expresses the ratio:

$$\varepsilon_{ex} = \frac{\dot{E}_p}{\dot{E}_F}$$
(20)

$\dot{E}_p = exergy\ rate\ of\ product\ in\ kW$

$\dot{E}_F = rate\ of\ fuel\ exergy\ supplied\ to\ a\ component\ in\ a\ system\ in\ kW$

For the power cycles, the product is the electricity produced, and the fuel is the geothermal fluid. Therefore, exegetic efficiency of the cycle can be represented by equation 21, shown below:

$$\varepsilon_{ex} = \frac{\dot{W}_{Net}}{\dot{E}_1} \tag{21}$$

3.2 Costs estimates

Cost estimation for major plant equipment such as the turbine, heat exchanger, condenser, pumps, and cooling tower is done in this work. These costs are referred here as purchased equipment cost (PEC) of the respective components.

Purchase equipment cost can be determined by referring to already purchased equipment of similar type. Since prices of equipment change over time due to different economic factors, the best cost of an equipment should be obtained directly from the vendor's quotation. However, this is usually difficult especially in academic research cases.

In situations where similar equipment with different size has been bought before, the cost of a new component can be established using the reference equipment. Different scaling factors are provided in the literature for the cost and size relationship shown in equation 22 below. In case the scaling factor cannot be found the rule of thumb is to use 0.6. Thus, the rule is most often referred to as six tenth rule. Equation 22 below is used to determine the cost of an equipment; C_x of a known size given the cost C_o and size S_o of a similar equipment.

$$C_x = C_o * \left(\frac{S_x}{S_o}\right)^{\propto} \tag{22}$$

Another technique used in cost estimation is the factorial cost technique. It employs technical specification of various key equipment of the system to estimate their costs [39]. For example, the cost of the turbine can be estimated using a cost equation that involves the net-work output as one of its input variables or say the cost of the heat exchanger can be estimated from the heat exchanger cost equation using the area and/or pressure drop as input variable(s).

Cost value used in this study have been extracted from available online literature referring to previous projects. It is known that the price of equipment changes over time due to different factors such as technological advancement, inflation, or deflation. To account for the changes, cost indices are used. The indices are usually published by different organizations or the government. In this thesis, Marshal and Swift equipment cost indices are used. To convert the past cost to current cost, the following equation is used:

$$PC_x = PC_o * \left(\frac{CI_x}{CI_o}\right) \tag{23}$$

Accuracy of costs estimates depends on the level of detail the project is in and aggregation of the system. Therefore, the analysis in this thesis tries to determine the costs of each individual component rather than estimating the cost of the whole system.

In this thesis cost equations have been used to determine the purchased equipment costs of different key equipment for the power cycles designed above. Cost equations are useful in that they give rough estimates of the costs of equipment. They are also key inputs in the optimization model that will be simulated in MATLAB.

3.2.1 Purchased equipment cost for an evaporator.

Referring to the literature by Bina ,et al 2017, the purchasing equipment cost of the evaporator; $PEC_{ev.}$ is given by equation 24 below[30]. The area of the evaporator; A_{ev} is given in meter square SI units. The cost is in 2017 USD.

$$PEC_{ev.} = 1397 * A_{ev}{}^{0.89} \qquad (24)$$

3.2.2 Purchased equipment cost for turbine.

The estimation of purchasing equipment cost for the turbine, PEC_T is done using an equation developed in a literature by Uma Maheswari et al.,2020 [40] .The turbine purchasing cost depends on the gross work output of the turbine as it can be seen in equation 25 below. The work output of the turbine; W_T is given in kW. The cost is in 2020 USD.

$$PEC_T = 4405 * W_T{}^{0.7} \qquad (25)$$

3.2.3 Purchased equipment cost for condenser.

Referring to the literature by Pourpasha ,et al 2020[41], the purchasing equipment cost of the condenser; $PEC_{cond.}$ is given by equation 26 below. With reference to figure 9 above, the mass flow rate entering the condenser; $\dot{m}_5$ is given in kg/s units. The cost is in 2020 USD.

$$PEC_{cond.} = 1773 * \dot{m}_5 \qquad (26)$$

3.2.4 Purchased equipment cost for pump.

The purchased equipment cost for the pump, PEC_P depends on the parasitic load of the pump, W_P. The power consumed by the pump is assumed to have been extracted from the turbine power produced by the given cycle. The equation was developed in a paper by Hassan et all,2020[36]. The work of the pump is in kW. The cost is in 2020 USD.

$$PEC_P = 1120 * W_P{}^{0.8} \qquad (27)$$

3.2.5 Purchased equipment cost for preheater.

Referring to the literature by Bina ,et al 2017[42], the purchasing equipment cost of the preheater; $PEC_{ph.}$ is given by equation 28 below. The area of the preheater; A_{ph} is given in square meters. The cost is in 2017 USD.

$$PEC_{ph} = 2143 * A_{ph}{}^{0.514} \qquad (28)$$

3.2.6 Purchased equipment cost for cooling tower.

A variable frequency drive cooling water fan is expected to be employed in the cooling tower to control mass flow rate of water entering the condenser from the cooling fan. The variation is mainly due to the variations in ambient air temperature in the Ngozi region. Through variable frequency drive pressure of the condenser is maintained[43]. This is done by adjusting the mass flow rate of cooling water (or air) when there is variation in ambient air temperature.

The purchased equipment cost for the cooling tower; PEC_{CT} represented by equation 29 below, is obtained from a literature by Velasquez B.[44]. The flow rate of the cooling tower; Q should be in kgal/min. The cost is obtained will be in 2010 KUSD.

$$PEC_{CT} = 164 * f * Q^{0.61} \qquad (29)$$

Another variable in the equation above is the cost scaling factor; f . Couper et al [45], gives values for the cost scaling factor given different value of range of cooling by the coolant from the cooling tower. For the case of the cycles designed in this thesis the cooling range is 15 degrees centigrade and the given cost scaling factor is 2.

3.2.7 Purchased equipment cost for generator.

The generator converts mechanical power from the turbine into electricity. Purchased equipment cost for the generator; PEC_g represented by equation 30 below, is obtained from a paper written by Lemmens,2016 [39]. The work of the generator; W_g should be in kW. The cost is in 2016 Euros.

$$PEC_g = 1,850,000 * \left[\frac{W_g}{11,800}\right]^{0.94} \qquad (30)$$

In 2016 USD, equation 30 above becomes

$$PEC_g = 2,059,050 * \left[\frac{W_g}{11,800}\right]^{0.94} \qquad (31)$$

3.2.8 Purchasing equipment cost for the Separator.

Geothermal separators are usually of two types: the horizontal and vertical separators. In recent years, horizontal separators have been more common in geothermal fields, especially in Iceland. Among other reasons for increased use of horizontal separators is the fact that they can be installed easily compared to vertical ones. Size limitation of vertical separators makes then difficult to handle. However vertical separators offer more quality steam compared to horizontal separators[27]. In this thesis vertical separators were employed.

There are different patterns in which the separator and the steam gathering system can be connected. For the case of the Ngozi project a steam gathering system is planned to be built from the wells, that will be connected to a pipe leading to the separator. The separator will be located close to the power plant.

Velasquez B [44], gives the cost equation for the purchased equipment cost for the separator; PEC_{sp} represented by equation 32 below. The value of Q is in kilo SCFM. The value is in 2010 KUSD.

$$PEC_{sp} = 0.79 * Q^{0.91} \tag{32}$$

When the fluid being used is under pressure close to or greater than 10 bars, another factor called the compressibility factor must be considered. Since some well head pressure values are above 10 bars as shown in table 2 above, then the compressibility factor should be considered. Z values can be obtained from compressibility charts; Figure 16 below:
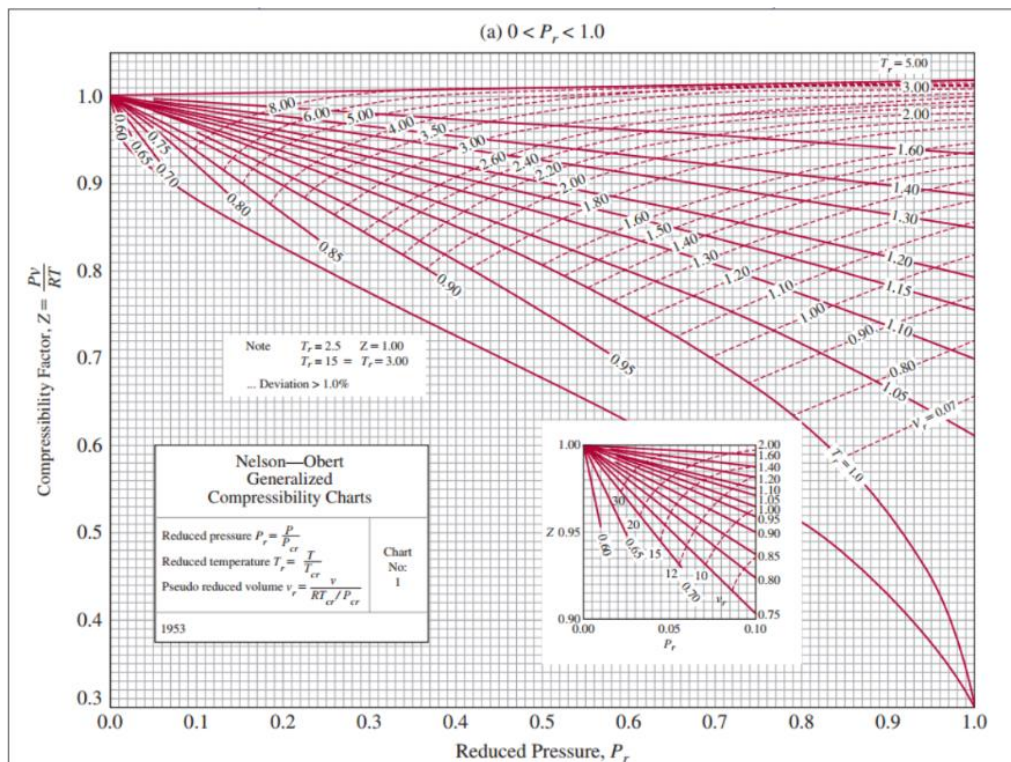
FIGURE 16: compressibility chart [46]

As it can be observed from the figure 16, to obtain Z, it is required to know the reduced temperature; T_r and reduced pressure value; P_r values. The values are calculated using equation 33 and equation 34 below. Critical temperature of water 374 degrees centigrade and critical pressure of water is 220 bar.

$$P_r = \frac{P}{P_c} \tag{33}$$

$$T_r = \frac{T}{T_c} \tag{34}$$

After calculating the Z value, equation 35 below is used to calculate the flow rate of geothermal water in cubic feet per minute.

$$SCFM = \frac{ACFM * \frac{T_{ST}}{T} * \frac{P}{P_{SP}}}{Z} \qquad (35)$$

3.2.9 Drilling costs

Drilling costs analysed in this thesis are made up of two components: the capital investment cost (drilling cost) for either production well or reinjection well and the operation and maintenance cost of the wells. The plan is to drill 3 slim wells to a total vertical depth of 1500m. Assuming two slim holes will be production wells and one slim well will be drilled for the reinjection. Similarly, if full size wells are used in exploration drilling, 3 wells would be drilled.

Slim well drilling cost is around USD 1.5 million. Full size well drilling cost used in this thesis is USD 6 million. The operation and maintenance cost is estimated as 2%-3% of the drilling cost[44]. In this work, 2% of the drilling cost will be assumed as operation and maintenance cost. The difference in diameters between slim wells does not change their drilling cost significantly since minor adjustments in drilling bit and casing are needed. The drilling rig is still the same. The difference arises in the thermodynamic part where different wellbores diameters result in different characteristic curves with different mass flow rates and enthalpies as shown in table 2 above. This also applies for different full size wellbore diameters considered here.

However, the costs cannot be used directly. They must be dispersed over the plant operating life also referred here as the plant economic life. According to assumptions made in section 2.2 above; the plant economic life is 20 years. Also, the cost must account for the effect of inflation (or deflation) as well as escalation in the market. A factor called constant escalation levelization factor; $CELF$ is used to take account of all these economic events in the marketplace. CELF is given by the equation 36 below:

$$CELF = \left(\frac{k(1 - k^n)}{1 - k}\right) * CRF \qquad (36)$$

But,

$$k = \frac{1 - r_n}{1 + i_{eff}} \qquad (37)$$

Also,

$$CRF = i_{eff} * \frac{(1 + i_{eff})^n}{(1 + i_{eff})^n - 1} \qquad (38)$$

Using equations 36,37 and 38 above, drilling cost; $\dot{Z}_{drill}$ In million USD can be calculated as follow:

$$\dot{Z}_{drill} = \dot{Z}_{drill,CI} + \dot{Z}_{drill,O\&M} \qquad (39)$$

Where:

$$\dot{Z}_{drill,CI} = 1.5 * \left(\frac{CELF}{3600 * N}\right) \qquad (40)$$

Also, the operation and maintenance cost of the drilled wells will be calculated as

$$\dot{Z}_{drill,O\&M.} = 0.02 * \dot{Z}_{drill,CI} \qquad (41)$$

3.2.10 Operation and maintenance cost for the equipment

Other than purchased equipment cost, all the equipment will need to be maintained over the life of the project so that they can function properly. The operation and maintenance cost rate denoted as $\dot{Z}_{k,OM}$ is calculated for each component. The operation and maintenance cost rate are calculated using equation 42 below:

$$\dot{Z}_{k,OM} = 20\% * \dot{Z}_{k,CI} \tag{42}$$

But,

$$\dot{Z}_{k,CI} = \frac{CELF * PEC_k}{3600 * N} \tag{43}$$

3.3 Thermo-economic analysis

Thermo-economics involves the combined analysis of both the thermodynamics and economics of the cycles. It involves determination of cost of each exergy streams in the thermodynamic cycle, identifying streams with cost inefficiencies so that thermodynamic improvements can be made. These improvements may eventually lead to the improvement of the overall cycle efficiency.

Traditionally, decisions to buy an equipment such as a turbine has been based on thermodynamic analysis. This can lead to less cost-efficient purchases as the real sources of inefficiency in equipment can hardly be determined efficiently using this analysis method. In addition to thermodynamic analysis, it is very crucial to conduct thermo-economic analysis for geothermal power investment since the projects usually have high initial capital investment. Thus, getting the investment right is very important.

Thermo-economic analysis is very important as it captures important information that is missed in traditional thermodynamic analysis[37].One of the key issue ignored in the thermodynamic analysis is the exergy destruction due to irreversibility. Result of the analysis are expected to determine the cost of the final product of the cycles that is the unit cost of electricity. This will show us how this compares to the market prices of other sources of electricity production including other renewables in the Tanzanian energy market.

The fundamental equation used in the thermo-economic analysis is the cost balance equation presented below. For each component in the power cycle, the sum of cost rates of exiting streams is equal to the sum of cost rates of entering streams and the operation and maintenance cost for the given component minus the exergy loss cost rate [37]. The equation is applied under the assumption that there is no heat transfer between the environment and the system.

$$\sum \dot{C}_o = \sum \dot{C}_i - \dot{C}_L + \dot{Z}_K \tag{44}$$

It is important to note that cost rate of any given stream in the cycle is the product of cost per unit exergy of that stream; c and exergy rate of the stream, $\dot{E}$ as shown in equations 45 and 46 below. Also, the component $\dot{Z}_K$ is made up of the capital investment cos rate and the operation and maintenance cost rate a s shown in equation 47 below.

$$\dot{C}_o = c_o * E_o \tag{45}$$

$$\dot{C}_i = c_i * E_i \tag{46}$$

$$\dot{Z}_K = \dot{Z}_{CI} + \dot{Z}_{OM} \tag{47}$$

In practice the cost rate for exergy loss; $\dot{C}_L$ is usually assumed zero for all streams except the ones that release their product(s) to the environment. This is because the exergy loss in thermo systems is usually applied to the entire system during design instead of individual components[37]. Generally, for costing purposes exergy losses for individual components are included in exergy destruction. Therefore, rate of exergy loss is zero:

$$\sum \dot{C}_L = 0 \tag{48}$$

Thus equation 44 above becomes:

$$\sum \dot{C}_o = \sum \dot{C}_i + \dot{Z}_K \tag{49}$$

However, for exiting streams that need further processing, such as reinjection or scrubbing before releasing to the environment, their cost per unit exergy can be expressed as shown in equation 50 below. According to Adrian Bejan [37], whenever extra costs are incurred in disposing a certain stream to the surroundings, these costs should be incorporated in the system that is under consideration .

$$c_{exit,k} = -\frac{\dot{C}_{exit,k}}{\dot{E}_{exit,k}} \tag{50}$$

The following sections look at the exergy balance equations for each component of the power cycles making use of the thermo-economic equation established above. The thermo-economic modelling is presented for each thermodynamic cycle proposed.

3.3.1 Modelling for the single flash cycle

Thermo economic modelling for the single flash cycle refers to figure 9 above. In the figure there are various streams that flow into and out of the key components of the cycle. The cost rate of these streams, cost per unit exergy as well as capital investment and operation and maintenance costs are analysed thermo-economically using cost rate balance equation as discussed below:

- **Stream from production well**:

The only stream looked at is the outflow from the well. The cost of drilling a slim well will be USD 1.5 m while the cost for drilling a full size well is assumed to be USD 6 m as discussed previously. This will include infrastructure that is; the drilling pad rig move and handling of drilling wastes.

$$\dot{C}_1 = \dot{Z}_{pw} \tag{51}$$

Since two (2) production slim holes are expected to be drilled, and considering the operation and maintenance cost of the slim holes, then $\dot{Z}_{pw}$ above becomes:

$$\dot{Z}_{pw} = 2 * (\dot{Z}_{pw,drill.} + \dot{Z}_{pw,O\&M}) \tag{52}$$

Substituting equation 52 into equation 51 and referring to the definition of cost rate in equation 45 above:

$$c_1 = \frac{2 * (\dot{Z}_{pw,drill.} + \dot{Z}_{pw,O\&M})}{\dot{E}_1} \tag{53}$$

- **Stream through the throttle valve:**

The throttle valve is used to regulate the separation pressure which is an important parameter in the optimization process of the power cycles as will be seen later.

$$\dot{C}_2 = \dot{C}_1 \tag{54}$$

Therefore,

$$c_2 = \frac{c_1 \dot{E}_1}{\dot{E}_2} \tag{55}$$

- **Stream flowing through the separator.**

Form the throttling valve where separation pressure is regulated, geothermal fluid flows into the separator. Here the two-phase geothermal fluid is separated into steam phase that goes into the turbine for power production and the condensate which is disposed to the reinjection well. The cost rate equations are as follows:

$$\dot{C}_3 + \dot{C}_4 = \dot{C}_2 + \dot{Z}_{sp} \tag{56}$$

$$c_3 \dot{E}_3 + c_4 \dot{E}_4 = c_2 \dot{E}_2 + \dot{Z}_{sp} \tag{57}$$

$\dot{Z}_{sp} = cost\ for\ puchasing\ the\ separator\ plus\ its\ operation\ and\ maintainace\ cost$

But,

$$\dot{Z}_{sp} = P\dot{E}C_{sp} + \dot{Z}_{sp,O\&M} \tag{58}$$

Substituting equation 58 into equation 57:

$$c_3 \dot{E}_3 + c_4 \dot{E}_4 = c_2 \dot{E}_2 + (P\dot{E}C_{sp} + \dot{Z}_{sp,O\&M}) \tag{59}$$

Since no exergy is added to the separator during the separation process, the cost per unit exergy of the products produced by the separator should be equal[37].
Therefore:

$$\frac{\dot{C}_3 - \dot{C}_2}{\dot{E}_3 - \dot{E}_2} = \frac{\dot{C}_4 - \dot{C}_2}{\dot{E}_4 - \dot{E}_2} \tag{60}$$

- **Streams flowing through the turbine.**

Only one stream; stream 3 flows to the turbine. Stream 5 flows from the turbine at the same time work is produced from the turbine.

$$\dot{C}_5 + \dot{C}_{W_T} = \dot{C}_3 + \dot{Z}_T \tag{61}$$

But

$$\dot{Z}_T = P\dot{E}C_T + \dot{Z}_{T,O\&M} \tag{62}$$

Substituting equation 62 into equation 61:

$$c_5 \dot{E}_5 + c_w \dot{W}_T = c_3 \dot{E}_3 + (P\dot{E}C_T + \dot{Z}_{T,O\&M}) \tag{63}$$

There are 2 unknowns, in equation 63 above, therefore another auxiliary equation is needed. The cost per exergy of steam entering the turbine is equal to the cost per exergy of saturated

liquid leaving the turbine. This is because there is no exergy added in the turbine[37]. Therefore,

$$c_3 = c_5 \tag{64}$$

From equation 63 above:

$$c_w = \frac{c_3(\dot{E}_3 - \dot{E}_5) + (P\dot{E}C_T + \dot{Z}_{T,O\&M})}{\dot{W}_T} \tag{65}$$

- **Stream through the condenser**

$$\dot{C}_6 + \dot{C}_{22} = \dot{C}_5 + \dot{C}_{21} + \dot{Z}_{cond} \tag{66}$$

But:

$$\dot{Z}_{cond} = P\dot{E}C_{cond} + \dot{Z}_{cond,O\&M} \tag{67}$$

Substituting equation 67 into Equation 66:

$$c_6\dot{E}_6 + c_{22}\dot{E}_{22} = c_5\dot{E}_5 + c_{21}\dot{E}_{21} + (P\dot{E}C_{cond} + \dot{Z}_{cond,O\&M}) \tag{68}$$

From exergy analysis of the power cycle, stream 21 is the cooling water stream from the cooling tower. Since water is assumed to be abundantly present in the environment, then its exergy is zero with reference to the environment. Thus,

$$\dot{E}_{21} = 0 \tag{69}$$

Also, another auxiliary equation is needed since there is one equation and two unknowns. At the condenser, the hot stream will transfer its exergy to the cold stream. The cost per unit exergy of the hot stream side remains constant[37].Therefore;

$$c_5 = c_6 \tag{70}$$

Substituting equation 69 and equation 70 above, into equation 68:

$$c_{22} = \frac{c_5(\dot{E}_5 - \dot{E}_6) + (P\dot{E}C_{cond} + \dot{Z}_{cond,O\&M})}{\dot{E}_{22}} \tag{71}$$

- **Overall plant streams analysis**

After analysing individual streams, it is time to evaluate the overall plant streams to determine the overall plant cost and unit cost of the product that is unit cost of electricity. Referring to figure 9 of the single flash cycle design, stream 6 is considered to have accounted for all the cost rates downstream. The cost of work output produced by the turbine is also added to the total cost equation. There are also other costs that are not included in the streams' costs such as the cost of the generator. These are included in the cost rate for supplementary; $\dot{C}_{supplementary}$. Therefore:

$$\dot{C}_{total} = \dot{C}_6 + \dot{C}_{W_T} + \dot{C}_{supplementary} \tag{72}$$

Also, the net-work output of the turbine; $\dot{W}_{net}$ is given by equation 73 below:

$$\dot{W}_{net} = \dot{W}_T - \dot{W}_{Parasitic\ load} \tag{73}$$

The cycles are designed with the aim of producing maximum amount of power. Electric power is the desired product, and the goal is to determine the cost of producing a unit of electricity. Therefore, the cost of a unit of electricity can be calculated using equation 72 and equation 73 above as follows:

$$c_e = \frac{\dot{C}_{total} * 7884 \, ^h/_{yr} * 3600 \, ^s/_h}{\dot{W}_{net} * 7884 \, ^h/_{yr}} \tag{74}$$

Therefore, the final equation for unit cost of electricity becomes:

$$c_e = \frac{3600 * \dot{C}_{total}}{\dot{W}_{net}} \tag{75}$$

3.3.2 Modelling for the Binary cycle

In this thesis, the binary cycle is designed with isopentane as the working fluid and the geothermal fluid as the source of heat. Like nuclear power cycle, the fluid used in the binary plant works in a closed cycle[47].Therefore, isopentane in figure 11 flows in a closed cycle. All the exergy and costs gained by the isopentane is assumed to have been extracted from the geofluid. The cost balance equations are as presented here below.

- **Stream from geothermal production well**

There is only one stream from the geothermal production well. The cost of the well is as discussed above. Equation 51 and equation 52 also apply here. The value of the cost per unit exergy of the stream from the production well; c_1 is given by equation 53 above.

Also, for the heat exchanger (preheater and evaporator) on the hot end, the cost per unit exergy will not change when the fluid passes through the hot side of the heat exchanger[37]. Therefore:

$$c_2 = c_1 \tag{76}$$

Also,

$$c_3 = c_2 \tag{77}$$

- **Streams through the preheater**

The cost balance equation for the preheater is given as:

$$\dot{C}_3 + \dot{C}_{11} = \dot{C}_2 + \dot{C}_{14} + \dot{Z}_{PH} \tag{78}$$

But

$$\dot{Z}_{PH} = P\dot{E}C_{PH} + \dot{Z}_{PH,O\&M} \tag{79}$$

substituting equation 79 into equation 78:

$$c_3\dot{E}_3 + c_{11}\dot{E}_{11} = c_2\dot{E}_2 + c_{14}\dot{E}_{14} + (P\dot{E}C_{PH} + \dot{Z}_{PH,O\&M}) \tag{80}$$

- **Streams through the evaporator**

Organic Rankine cycles design includes heat exchangers. In this cycle heat exchangers contribute significantly in the operating cost[36].

$$\dot{C}_2 + \dot{C}_{10} = \dot{C}_1 + \dot{C}_{11} + \dot{Z}_{EV} \tag{81}$$

Therefore,

$$c_2\dot{E}_2 + c_{10}\dot{E}_{10} = c_1\dot{E}_1 + c_{11}\dot{E}_{11} + \dot{Z}_{EV} \tag{82}$$

But

$$\dot{Z}_{EV} = P\dot{E}C_{EV} + \dot{Z}_{EV,O\&M} \tag{83}$$

Substituting equation 83 into equation 82 and referring to equation 76, the final equation becomes:

$$c_{10}\dot{E}_{10} - c_{11}\dot{E}_{11} = c_1(\dot{E}_1 - \dot{E}_2) + (P\dot{E}C_{EV} + \dot{Z}_{EV,O\&M}) \tag{84}$$

- **Streams through the turbine**

$$\dot{C}_{12} + \dot{C}_{W_T} = \dot{C}_{10} + \dot{Z}_T \tag{85}$$

Thus,

$$c_{12}\dot{E}_{12} + c_w\dot{W}_T = c_{10}\dot{E}_{10} + \dot{Z}_T \tag{86}$$

The reasoning behind the establishment of equation 64 above also apply here, thus

$$c_{10} = c_{12} \tag{87}$$

Substituting equation 87 into equation 86 and referring to equation 62, the final equation becomes:

$$c_{12}(\dot{E}_{12} - \dot{E}_{10}) + c_w\dot{W}_T = P\dot{E}C_T + \dot{Z}_{T,O\&M} \tag{88}$$

- **Stream through the condenser**

$$\dot{C}_{22} + \dot{C}_{13} = \dot{C}_{21} + \dot{C}_{12} + \dot{Z}_{cond} \tag{89}$$

But $\dot{Z}_{cond}$ can also be expanded as shown in equation 67 above. Therefore equation 89 becomes:

$$c_{22}\dot{E}_{22} + c_{13}\dot{E}_{13} = c_{21}\dot{E}_{21} + c_{12}\dot{E}_{12} + (P\dot{E}C_{cond} + \dot{Z}_{cond,O\&M}) \tag{90}$$

From exergy analysis of the power cycle, stream 21 is the ambient air stream and is taken as the reference or dead state. That is its relative exergy is considered 0 as it was represented by equation 69 above. Also, the reasoning behind the establishment of equation 70 above also apply here, thus

$$c_{13} = c_{12} \tag{91}$$

Substituting equation 91 into equation 90:

$$c_{13}(\dot{E}_{13} - \dot{E}_{12}) + c_{22}\dot{E}_{22} = P\dot{E}C_{cond} + \dot{Z}_{cond,O\&M} \tag{92}$$

- **Working fluid through the pump**

$$\dot{C}_{14} = \dot{C}_{13} + \dot{C}_{W_P} + \dot{Z}_P \tag{93}$$

But

$$\dot{Z}_P = PEC_P + \dot{Z}_{P,O\&M} \tag{94}$$

Substituting equation 94 into equation 93:

$$c_{14}\dot{E}_{14} = c_{13}\dot{E}_{13} + c_p\dot{W}_P + (P\dot{E}C_P + \dot{Z}_{P,O\&M}) \tag{95}$$

Assuming the electric power consumed by the pump is supplied by the turbine, the cost per unit exergy of the pump; c_p will be equal to the cost per unit exergy for the turbine's work output; c_w

$$c_p = c_w \tag{96}$$

Therefore, the final equation becomes:

$$c_{14}\dot{E}_{14} - c_{13}\dot{E}_{13} - c_w\dot{W}_P = P\dot{E}C_P + \dot{Z}_{P,O\&M} \tag{97}$$

Solving the above equations, all the values(unknowns) can be obtained.

- **Overall plant streams analysis**

Referring to figure 11 of the binary cycle design. Since all the costs were transferred from the geofluid to working fluid, the cost rate of turbine output; $\dot{C}_{W_T}$ will carry all the costs of the cycle. The remaining costs will be accounted in the supplementary costs; $\dot{C}_{supplementary}$

$$\dot{C}_{total} = \dot{C}_{W_T} + \dot{C}_{supplementary} \tag{98}$$

Therefore, the cost of a unit of electricity can be calculated using equation 98 and equation 73 above as follows:

$$c_e = \frac{3600 * \dot{C}_{total}}{\dot{W}_{net}} \tag{99}$$

3.3.3 Modelling for the double flash cycle

Cost rate equations for the double flash turbine will have the same formation as the single flash turbine discussed above. The only difference will be that the double flash cycle has two sets of cost rate equations for turbine (high-pressure turbine, and the low-pressure turbine) and separator (high-pressure separator, and the low-pressure separator). Referring to figure 10 for the double flash cycle above, the cost balance equations for each stream are as presented here below:

- **Geothermal fluid from production well**

The only stream looked at is the outflow from the well. The cost flow equation is exactly like equation 53 above.

- **Stream through throttle valve before HPS**

The throttle valve is used to regulate the separation pressure which is an important parameter in the optimization process of the power cycles as will be seen later.

$$\dot{C}_2 = \dot{C}_1 \tag{100}$$

Therefore:

$$c_2 = \frac{c_1 \dot{E}_1}{\dot{E}_2} \tag{101}$$

- **Stream through the High-Pressure Separator (HPS)**

$$\dot{C}_3 + \dot{C}_4 = \dot{C}_2 + \dot{Z}_{HPS} \tag{102}$$

Where:

$\dot{Z}_{HPS} = cost\ rate\ for\ capital\ investment\ plus\ O\&M\ cost\ for\ HPS$

But

$$\dot{Z}_{HPS} = P\dot{E}C_{HPS} + \dot{Z}_{HPS,O\&M} \tag{103}$$

Substituting equation 103 into Equation 102:

$$c_3 \dot{E}_3 + c_4 \dot{E}_4 = c_2 \dot{E}_2 + (P\dot{E}C_{HPS} + \dot{Z}_{HPS,O\&M}) \tag{104}$$

The high-pressure separator analysis involves another auxiliary equation to solve for cost per unit exergy of stream 3; c_3 and cost per unit exergy of stream 4; c_4 .Since no exergy is added to the separator during the separation process, the cost per unit exergy of the products produced by the separator should be equal[37].

Therefore:

$$\frac{\dot{C}_3 - \dot{C}_2}{\dot{E}_3 - \dot{E}_2} = \frac{\dot{C}_4 - \dot{C}_2}{\dot{E}_4 - \dot{E}_2} \tag{105}$$

- **Stream through the High-Pressure Turbine (HPT)**

The high-pressure turbine has two outgoing cost streams, that is the cost rate associated with work of the turbine: $\dot{C}_{W_{HPT}}$ and the cost rate for stream 5. The only incoming stream is the

stream from the high-pressure separator that is stream 3. The cost balance equations are as shown here below:

$$\dot{C}_5 + \dot{C}_{W_{HPT}} = \dot{C}_3 + \dot{Z}_{HPT} \tag{106}$$

But

$$\dot{Z}_{HPT} = P\dot{E}C_{HPT} + \dot{Z}_{HPT,O\&M} \tag{107}$$

Substituting equation 107 into Equation 106:

$$c_5\dot{E}_5 + c_{HPT}\dot{W}_{HPT} = c_3\dot{E}_3 + (P\dot{E}C_{HPT} + \dot{Z}_{HPT,O\&M}) \tag{108}$$

There are three unknowns in equation 108 above, thus an additional auxiliary equation is required to solve for the unknowns. The same explanation used to establish equation 64 above is relevant for the double flash cycle too. Therefore, substituting equation 64 into equation 108:

$$c_{HPT} = \frac{c_3(\dot{E}_3 - \dot{E}_5) + (P\dot{E}C_{HPT} + \dot{Z}_{HPT,O\&M})}{\dot{W}_{HPT}} \tag{109}$$

- **Stream through throttle valve before LPS**

Stream 4 enters the valve where pressure is regulates resulting into stream 6. The cost balance equations are as follows:

$$\dot{C}_6 = \dot{C}_4 \tag{110}$$

Therefore:

$$c_6 = \frac{c_4\dot{E}_4}{\dot{E}_6} \tag{111}$$

- **Stream through Low Pressure Separator (LPS)**

Stream 6 enters the low-pressure separator, where it is flashed. Two streams emerge, stream 7 which is a saturated steam and stream 8 which is saturated liquid state. Stream 7 move to the LPT while stream 8 is reinjected back to the reservoir. The cost balance equations are as follows:

$$\dot{C}_7 + \dot{C}_8 = \dot{C}_6 + \dot{Z}_{LPS} \tag{112}$$

But

$$\dot{Z}_{LPS} = P\dot{E}C_{LPS} + \dot{Z}_{LPS,O\&M} \tag{113}$$

Substituting equation 113 into Equation 112:

$$c_7\dot{E}_7 + c_8\dot{E}_8 = c_6\dot{E}_6 + (P\dot{E}C_{LPS} + \dot{Z}_{LPS,O\&M}) \tag{114}$$

For the reasons explained in establishing equation 105 above, another auxiliary equation was established:

$$\frac{\dot{C}_7 - \dot{C}_6}{\dot{E}_7 - \dot{E}_6} = \frac{\dot{C}_8 - \dot{C}_6}{\dot{E}_8 - \dot{E}_6} \tag{115}$$

Solving equation 114 and equation 115 above the values of c_7 and c_8 can be obtained.

- **Stream through the Low-Pressure Turbine (LPT)**

$$\dot{C}_{10} + \dot{C}_{W_{LPT}} = \dot{C}_9 + \dot{Z}_{LPT} \tag{116}$$

But

$$\dot{Z}_{LPT} = P\dot{E}C_{LPT} + \dot{Z}_{LPT,O\&M} \tag{117}$$

Substituting equation 117 into Equation 116:

$$c_{10}\dot{E}_{10} + c_{LPT}\dot{W}_{LPT} = c_9\dot{E}_9 + (P\dot{E}C_{LPT} + \dot{Z}_{LPT,O\&M}) \tag{118}$$

Notice that there is a mixing of stream 5 and stream 7 before the entrance of the low-pressure turbine where:

$$\dot{C}_9 = \dot{C}_5 + \dot{C}_7 \tag{119}$$

Therefore,

$$c_9 = \frac{c_5\dot{E}_5 + c_7\dot{E}_7}{\dot{E}_9} \tag{120}$$

Also referring to discussions that led to in establishing equation 64 above, another auxiliary equation was established:

$$c_9 = c_{10} \tag{121}$$

Substituting equation 121 into Equation 118:

$$c_{LPT} = \frac{c_9(\dot{E}_9 - \dot{E}_{10}) + (P\dot{E}C_{LPT} + \dot{Z}_{LPT,O\&M})}{\dot{W}_{LPT}} \tag{122}$$

- **Stream through the condenser**

Streams flowing through the condenser include the fluid from the turbine, the inlet and outlet from the cooling tower and condensate to the pump. Their cost equations are as shown here below:

$$\dot{C}_{11} + \dot{C}_{22} = \dot{C}_{10} + \dot{C}_{21} + \dot{Z}_{cond} \tag{123}$$

$\dot{Z}_{cond}$ can be expanded in the same way as equation 67 above. Therefore equation 123 becomes:

$$c_{11}\dot{E}_{11} + c_{22}\dot{E}_{22} = c_{10}\dot{E}_{10} + c_{21}\dot{E}_{21} + (P\dot{E}C_{cond} + \dot{Z}_{cond,O\&M}) \tag{124}$$

Refer to explanation given in establishing equation 69 above. Also, the reasoning behind the establishment of equation 70 above also apply here, thus

$$c_{11} = c_{10} \qquad (125)$$

Thus equation 124 above becomes:

$$c_{22} = \frac{c_{10}(\dot{E}_{10} - \dot{E}_{11}) + (P\dot{E}C_{cond} + \dot{Z}_{cond,O\&M})}{\dot{E}_{22}} \qquad (126)$$

- **Overall plant streams analysis**

Referring to figure 10 of the double flash cycle design, stream 11 is considered to have accounted for all the cost rates downstream. The cost of work produced by both low pressure and high pressure the turbine is also added to total cost equation. There are also other costs that are not included in the streams' costs such as the cost of the generator. These are included in the cost rate for supplementary, $\dot{C}_{supplementary}$. Therefore:

$$\dot{C}_{total} = \dot{C}_{11} + \dot{C}_{W_{HPT}} + \dot{C}_{W_{LPT}} + \dot{C}_{supplementary} \qquad (127)$$

Also, the net-work output of the turbine; $\dot{W}_{net}$ is given by equation 128 below:

$$\dot{W}_{net} = W_{HPT} + \dot{W}_{LPT} - \dot{W}_{Parasitic\ load} \qquad (128)$$

Therefore, the cost of a unit of electricity can be calculated using equation 127 and equation 128 as follows:

$$c_e = \frac{3600 * \dot{C}_{total}}{\dot{W}_{net}} \qquad (129)$$

4   RESULTS AND DISCUSSION

As discussed in previous sections, slim wells are generally considered to have final drilled wellbore diameter of less than 6 inches (approximately 15 cm). Therefore, in this study the well bore diameters above 15 cm are assumed to be full size wells.

The present work assumes drilling costs to be an average of USD 1.5 million for all slim well with different diameters. The difference in diameters between slim wells does not change their drilling cost significantly since minor adjustments in drilling bit and casing are needed. The drilling rig is still the same. However, a difference is pressure vs flow rate arises due to change in thermodynamics and heat transfer characteristics due to change in wellbore diameter as shown in table 2 above. This also occurs for different full size wellbore diameters.

The present study was done for a liquid dominated geothermal field. The field is low enthalpy as shown by well testing data in table 2 above. It is important to mention assumptions used in the case study from the literature by Pritchett J. W. [25] used for the current modelling. The study assumes the boreholes to be drilled with the same(uniform) diameter to total vertical depth. Usually, geothermal wells are drilled in sections of decreasing diameter to total depth. Geothermal fluid properties are calculated assuming that the fluid has the properties equivalent to pure water. Moreover, the depth of the wells is around 1500 m. The results from the study are discussed below.

4.1   Work output from the power cycles.

Work produced by the power cycles is from the turbine. As discussed previously, some of the work output from the turbine is used to run pumps and the cooling tower fan. This is called parasitic load as it reduces the overall power output. Assuming the parasitic load is supplied by the turbine; the net-work output produced by the cycle is equal to the work output of the turbine minus parasitic loads.
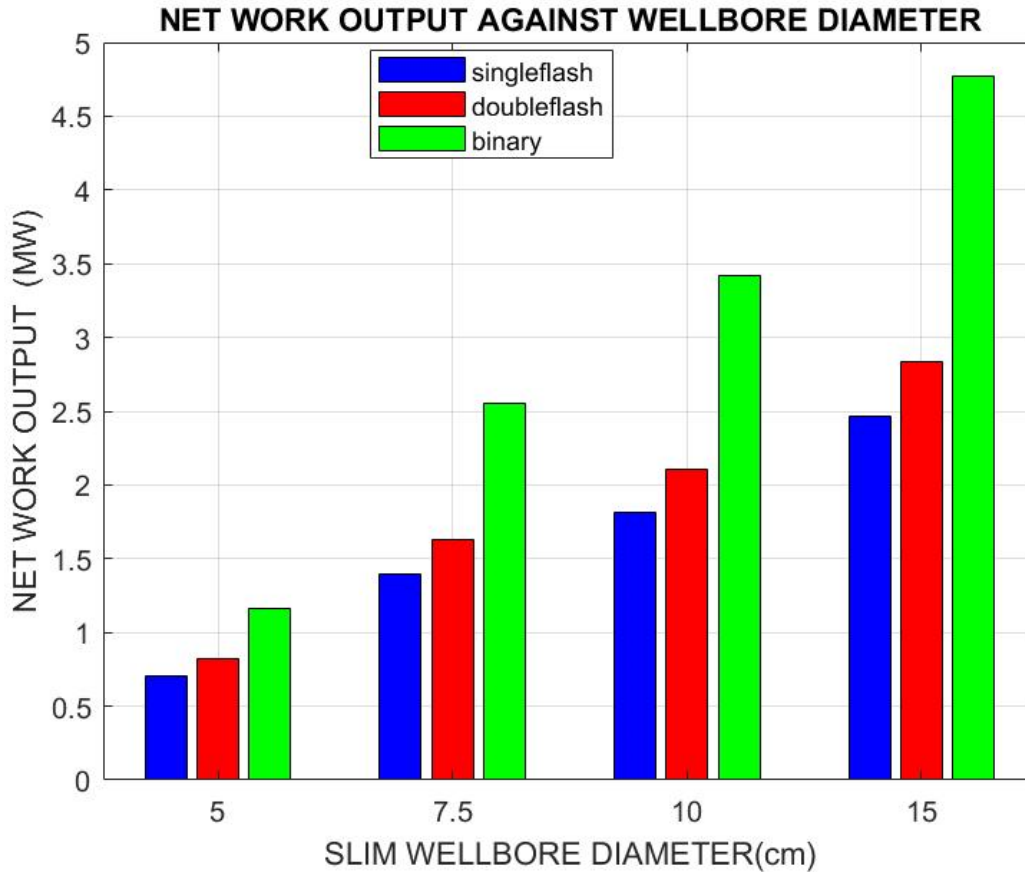
FIGURE 16: Net-work output for the three power cycles against slim wellbore diameter

Figure 16 above and figure 17 below show the net-work output generated by the three proposed power cycles for different slim wellbore diameters and full-size wellbore diameters respectively. The net-work of each power cycle is observed to be increasing as the wellbore diameter increases. The binary cycle produces the highest comparative net-work output when using either slim wells or full-size wells. Double flash power cycle has the next highest amount of net-work output followed by the single flash cycle.

The binary produces the highest power compared to the other power cycles for each wellbore diameter considered due to the nature of the fluid. As it has been mentioned above, the fluid is liquid dominated and low enthalpy. Single flash and double flash technologies involve a separation process. During the process only steam is sent to the turbine, a huge amount of energy is lost with the separated liquid brine. The power output can only be improved to a small extent by increasing the fluid flow rate by increasing the diameter. This results in more power produced by the binary plant compared to the others as seen from figure 16 and figure 17.
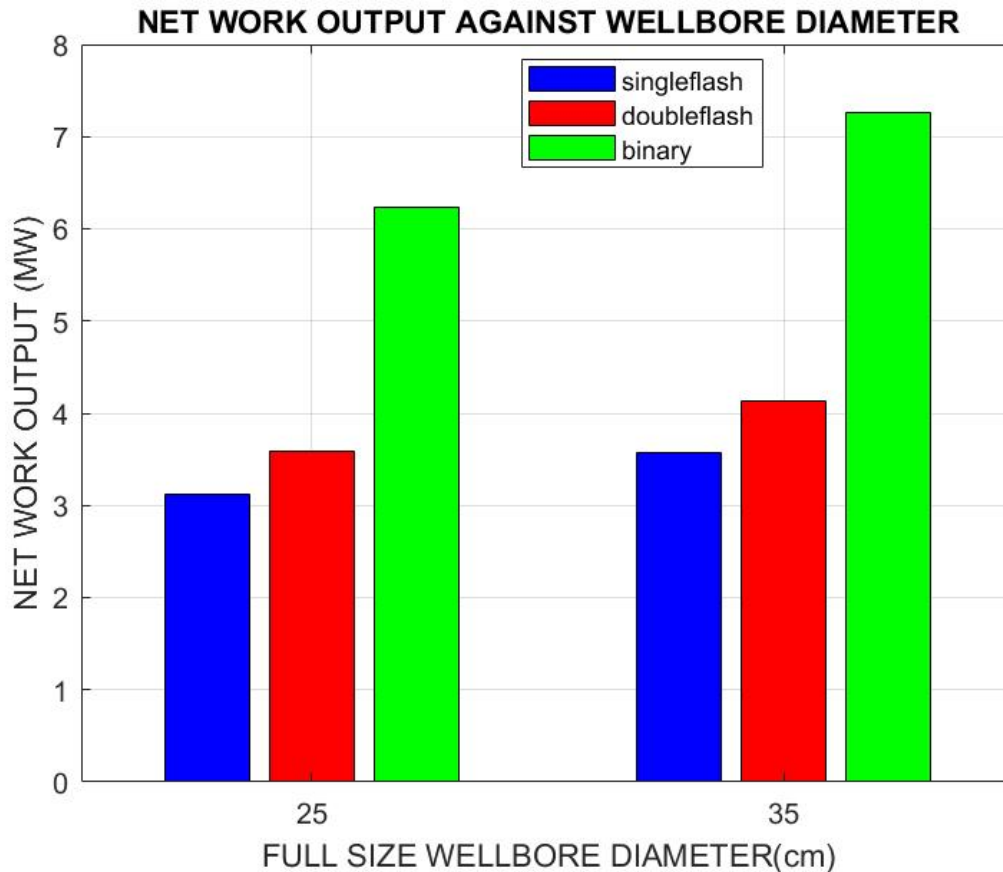
FIGURE 17: Net-work output for the three power cycles against full-size wellbore diameter

The increased well bore diameter results in the increase in discharge capacity of the wells. Therefore, increase in the amount of power produced is due to the increase in mass flow rate of the fluid that goes into the turbine.

Basing on the figure 16 above, 15 cm wellbore diameter slim wells would be more ideal for Ngozi project. Also, binary power plant would be the most suitable for power generation since the binary power cycle offers highest power output compared to other cycles.

4.2   Cost of unit of power

The cost of a unit of power is given by equation 75, equation 99 and equation 129 defined above. As seen from the above equations, the cost depends on the total cost of the streams and the net-work output produced by the power cycle under consideration.

 Figure 18 below shows the variations of the cost of the work output produced from the three different proposed power cycles against the slim wellbore diameter. As shown in the figure, the cost of work output decreases as the diameter of the slim wells increases. This is due to the increased net-work output as the wellbore diameter increases from 5 cm to 15 cm (figure 16 above), while the cost of the well remains unchanged. Slim well with wellbore diameter 15 cm has the lowest cost of work.
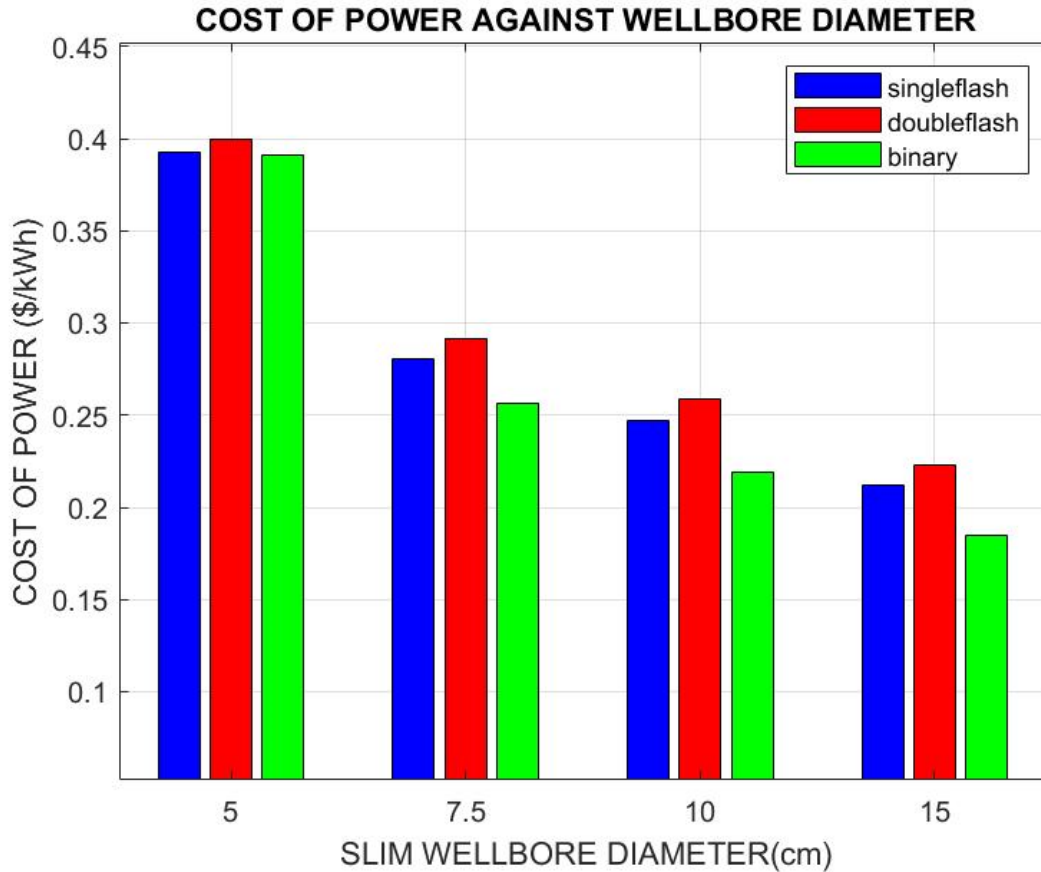
FIGURE 18: Cost of electricity against the wellbore diameter for slim wells

Also, it can be noticed from figure 19 below, for full size wells (well bore diameter greater than 15 cm); as the diameter of the wellbore increases from 25 cm to 35 cm, the cost of decreases with increasing diameter. This means, for a certain wellbore diameter between 25 cm and 35 cm the cost of power reached a highest value and then started to decrease. This is because the cost of drilling the full size well is initially too high to be compensated by the increase in net-work output. However, as the net-work output continues to increase as the wellbore diameter increases, the cost of a unit of work output starts to decrease due to economies of scale.
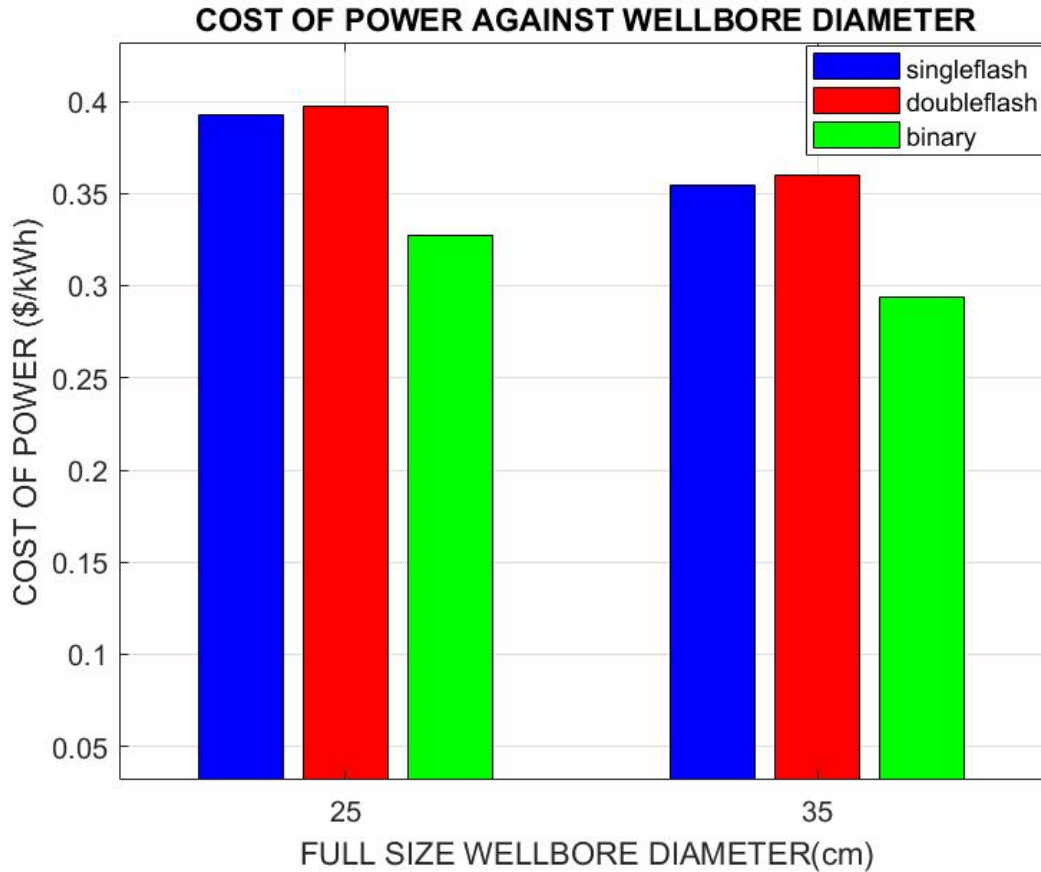
FIGURE 19: Cost of electricity against the wellbore diameter for full-size wells

It can be seen from figure 18 and figure 19 above that, in general, double flash power cycle has the highest cost per unit of power followed by single flash and then followed by the binary flash. Double flash cycle has the highest cost per unit of power despite having higher net-work produced compared to single flash cycle. This is mainly due to the high investment cost as well as operation and maintenance cost of the two turbines employed in double flash cycle. All the investment cost is recovered (charged) on each unit of power produced. The figures further confirm the suitability of binary cycle over the other proposed power cycles for the Ngozi project.

4.3   First and second law efficiency

The first law efficiency or thermal efficiency is the ratio of net-work to the heat supplied by the geofluid. Also, the second law efficiency or exegetic efficiency is the ratio of net-work to the exergy supplied by the geofluid. The metrics show how efficient the power cycles are in converting heat and exergy contained in the geofluid into electric power.
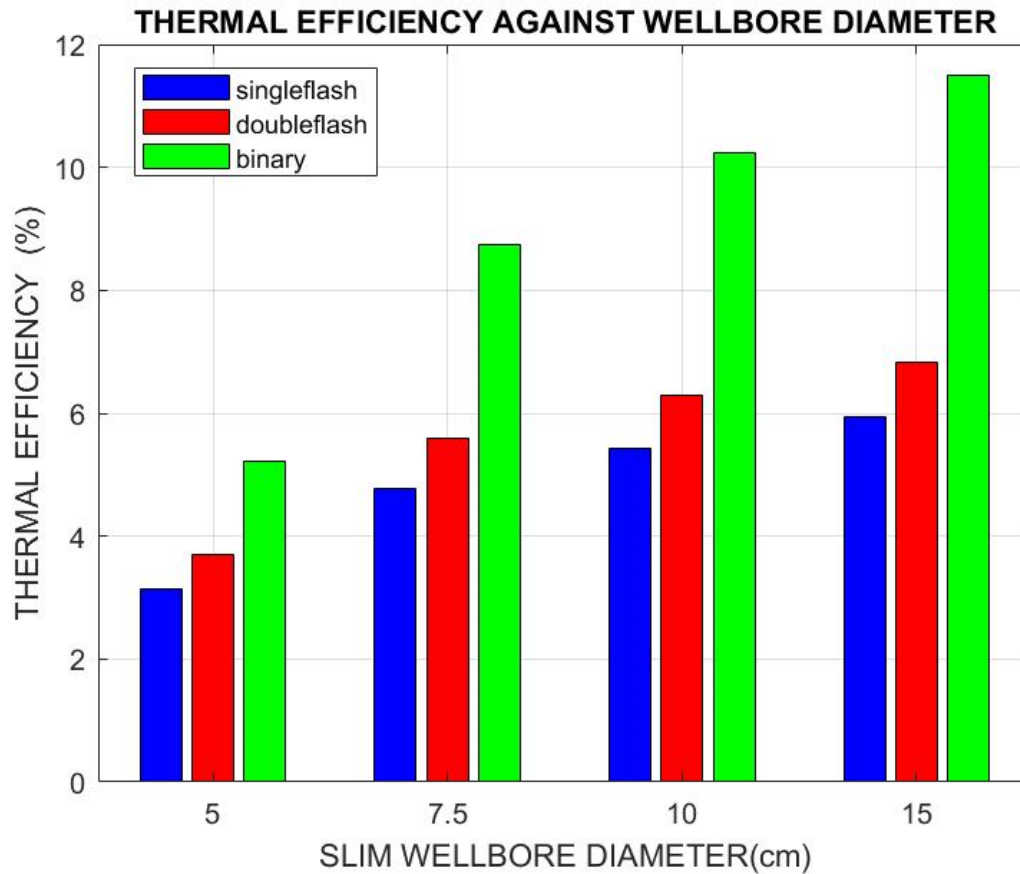
FIGURE 20: First law efficiency against slim wellbore diameter

Figure 20 above and figure 21 below, show thermal efficiency for different wellbore diameters for slim wells and full-size wells respectively. As can be seen in the figures, the binary cycle has the highest thermal and exegetic efficiencies. This is because binary cycle produces the highest net-work output as shown in figure 16 above. Following the binary cycle, the double flash cycle has the next highest values of efficiency and then followed by the single flash cycle. This trend agrees with the net-work output produced by the cycles as presented in figure 16 above.

The binary plant is expected to be more efficient than the rest of the plants since it enables heat transfer from the geothermal fluid to the working fluid with low boiling point, unlike the single and double flash plants where huge amount of heat is lost with the brine during the separation process as discussed earlier.
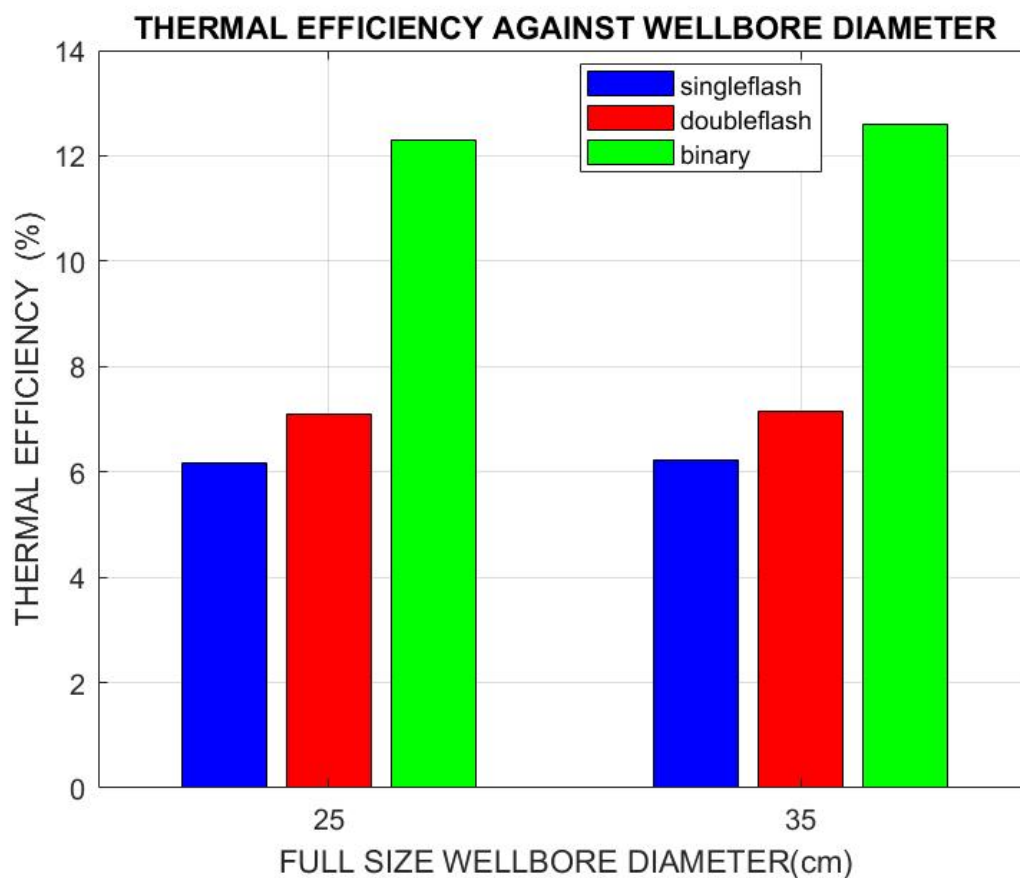
FIGURE 21: First law efficiency against full-size wellbore diameter

Figure 22 and figure 23 below, show the exergetic efficiency for different wellbore diameters for slim wells and full-size wells respectively. As it can be seen in the figures, the binary cycle has the highest second law efficiency. This is because binary cycle produces the highest net-work output as it can be seen in figure 16 above.

After the binary cycle, the double flash cycle follows with the higher values of efficiency and then followed by the single flash cycle. This trend agrees with the net-work output produced by the cycles as presented in figure 16 above.
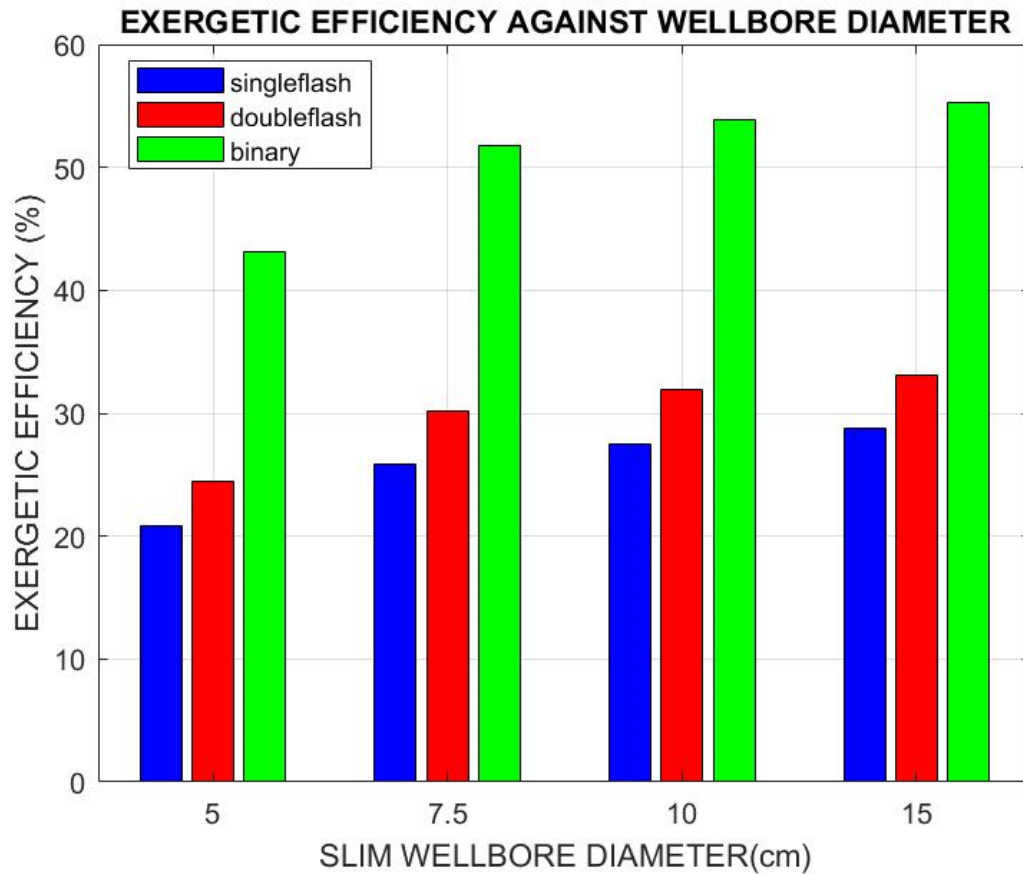
FIGURE 22: Second law efficiency against slim wellbore diameter

Both first and second law efficiencies for single flash cycle and double flash cycle do not increase significantly as the wellbore diameters increase. This is due to the nature of the geothermal fluid. The fluid is liquid dominated thus the increase in wellbore diameter hence mass flow rate has a minor effect on the increase in the mass of steam that flows into the turbine in the single flash and double flash cycles.
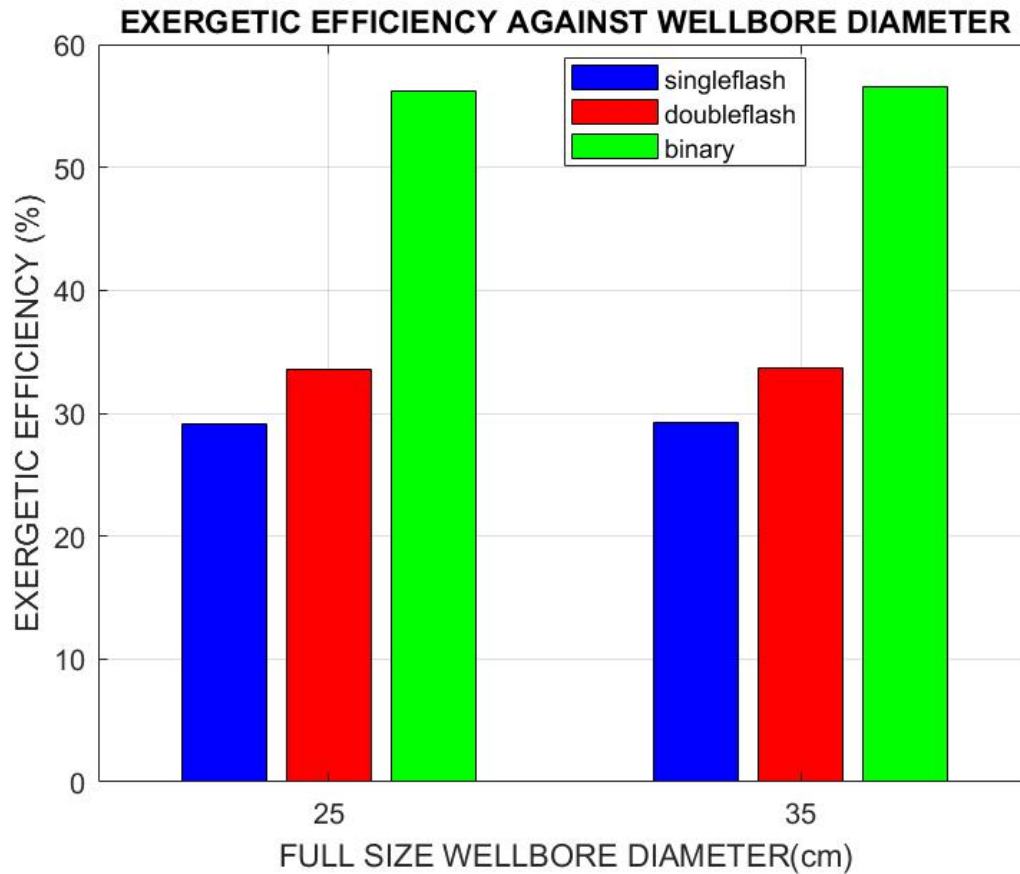
FIGURE 23: Second law efficiency against full-size wellbore diameter

4.4   Total cost per Megawatt

Figure 24 and figure 25 show the variation of total cost per megawatt against wellbore diameters for slim wells and full-size wells respectively. The total cost per megawatt decreases as the wellbore diameter increases.

The total cost per megawatt is the lowest for the binary plants, followed by single flash and then double flash. Again, binary flash has the highest net-work output (figure 16) compared to the rest of the cycles hence the total cost per MW is the lowest.
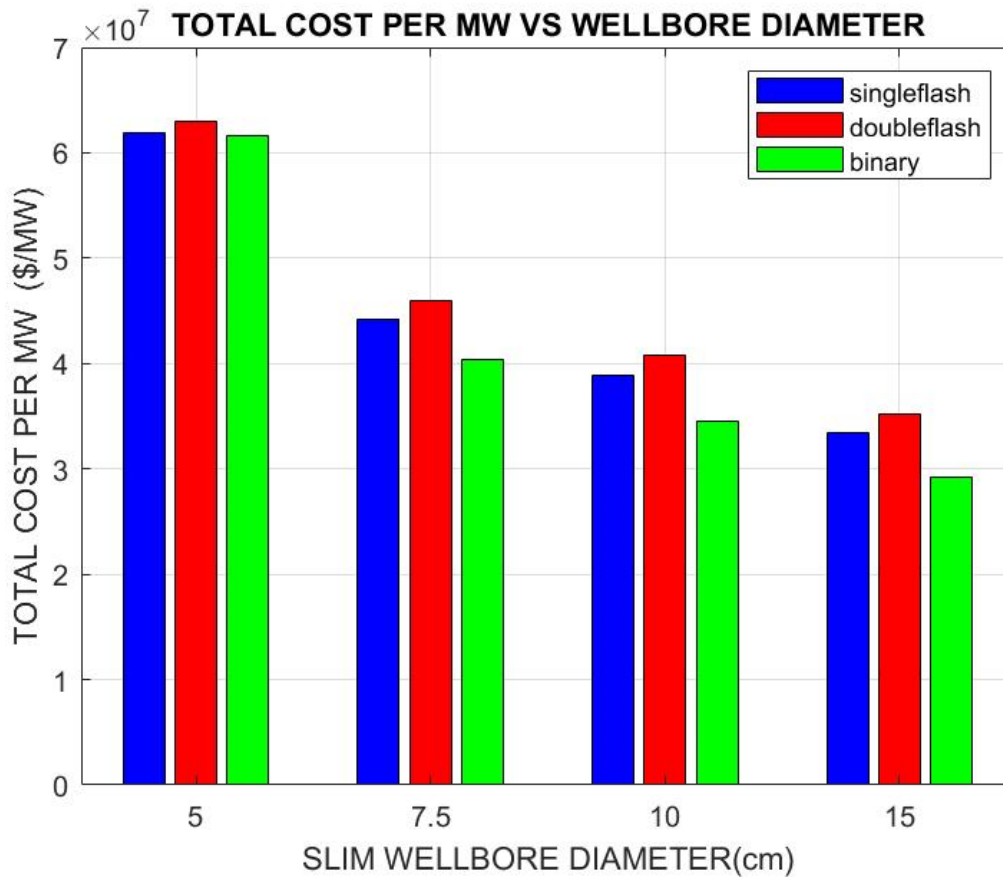
Figure 24: Total cost per MW against slim wellbore diameter.

Generally, the total cost per megawatt in each cycle decreases as the wellbore diameter increases. This is due to the general increase in net-work output produced by these wells as the mass flow rate increases as a result of increase in the wellbore diameter. From figure 24 above, it can be observed that double flash cycle has the highest value of total cost per megawatt. This is due to high investment cost in purchasing an additional turbine, which is not compensated by the slight increase in power.

For full-size wellbore diameter (that is 25 cm and 35 cm) the total cost per megawatt increases significantly compared to total cost per megawatt for slim wellbore as it can be seen in figure 25 below. This is due to the increased cost of drilling full-size wells compared to slim well drilling. However, as the diameter of the full size well continue increasing from 25 cm to 35 cm the amount of power also increases. This leads to decrease in total cost per megawatt. The trend is like the one observed in figure 18 and figure 19 above.
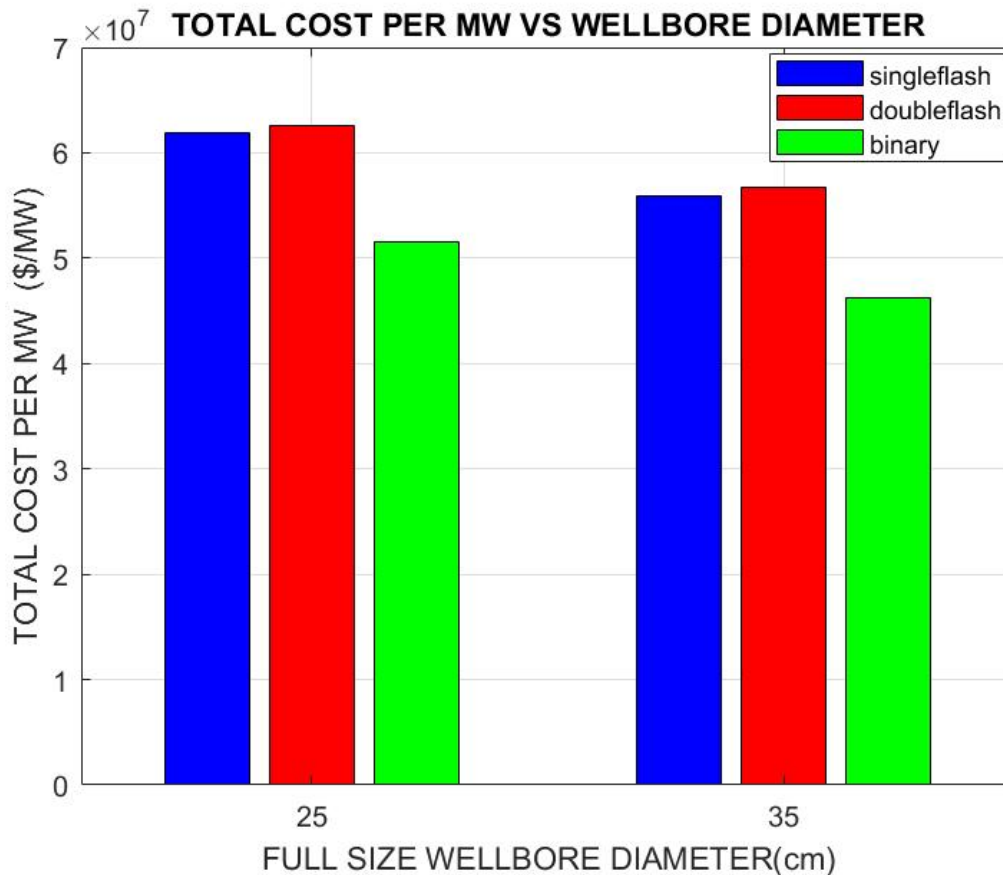
Figure 25: Total cost per MW against full-size wellbore diameter.

4.5   Project cash flow and Breakeven point

Cash flow for the project is represented by Figure 26 given below. The figure shows cash flow for three different size wells: one is a 15 cm slim wellbore and other two are 25 cm and 35 cm full-size wellbores. The analysis assumes that after drilling the wells, a binary power plant was implemented. The 15 cm slim well is selected because it offers the lowest cost of the unit of electricity as well as the highest power output. Moreover, binary power plant is the best choice according to the analysis above.

There are different business arrangements particularly concerning raising project's investment. Some projects get loans from banks, some get grants and some work on the combination of the two. In African perspective, for example, the early exploration activities are usually financed by African governments. Investors usually prefer not to take part at this stage. This is due to the high risk of geothermal projects in early stages. There have been some organisations such as the GRMF that have offered grants and loans in either cash terms or equity in the project so that they can finance exploration activities in the region. The use of grant for that matter would make more compelling business case (if available) instead of a loan.

When the project starts, a huge investment is made in drilling and purchase of the power plant equipment, so cash flow is very negative. Then, production starts, and revenue is generated by selling the electricity. The obtained sales revenue is used to pay off the debt. Since full size wells have higher drilling and equipment cost compared to slim wells, they have bigger initial investment and therefore more debt.

As discussed above, the electricity sector in Tanzania is a monopoly. The public utility company TANESCO controls the production, transmission, and distribution of electricity in the country. It is only in the generation where private sector is involved, but then the electricity produced should be sold to the state utility company for transmission and distribution. There are three types of producers (electricity generators) in Tanzania: renewable energy generators with power export capacity less than 10 MW referred to as Small Power Produces (SPP), the private electricity producers referred to as Independent Power Producers (IPP), and Public Private Partnership (PPP).

Usually, the utility company pays producers of power a wholesale price for the electricity they produce. This price is agreed between the two parties in the power purchase agreement. This price is lower than the market price since the market price should include extra charges such as transmission charges and taxes. In Tanzania, the wholesale price for SPP connected the national grid is 137.29 TZS /kWh (0.059 $/kWh) during rainy season and 183.05 TZS/kWh (0.079 $/kWh) during dry season[48]. For simplicity in revenue calculations, the average of the two prices will be used which is 0.069 $/kWh.
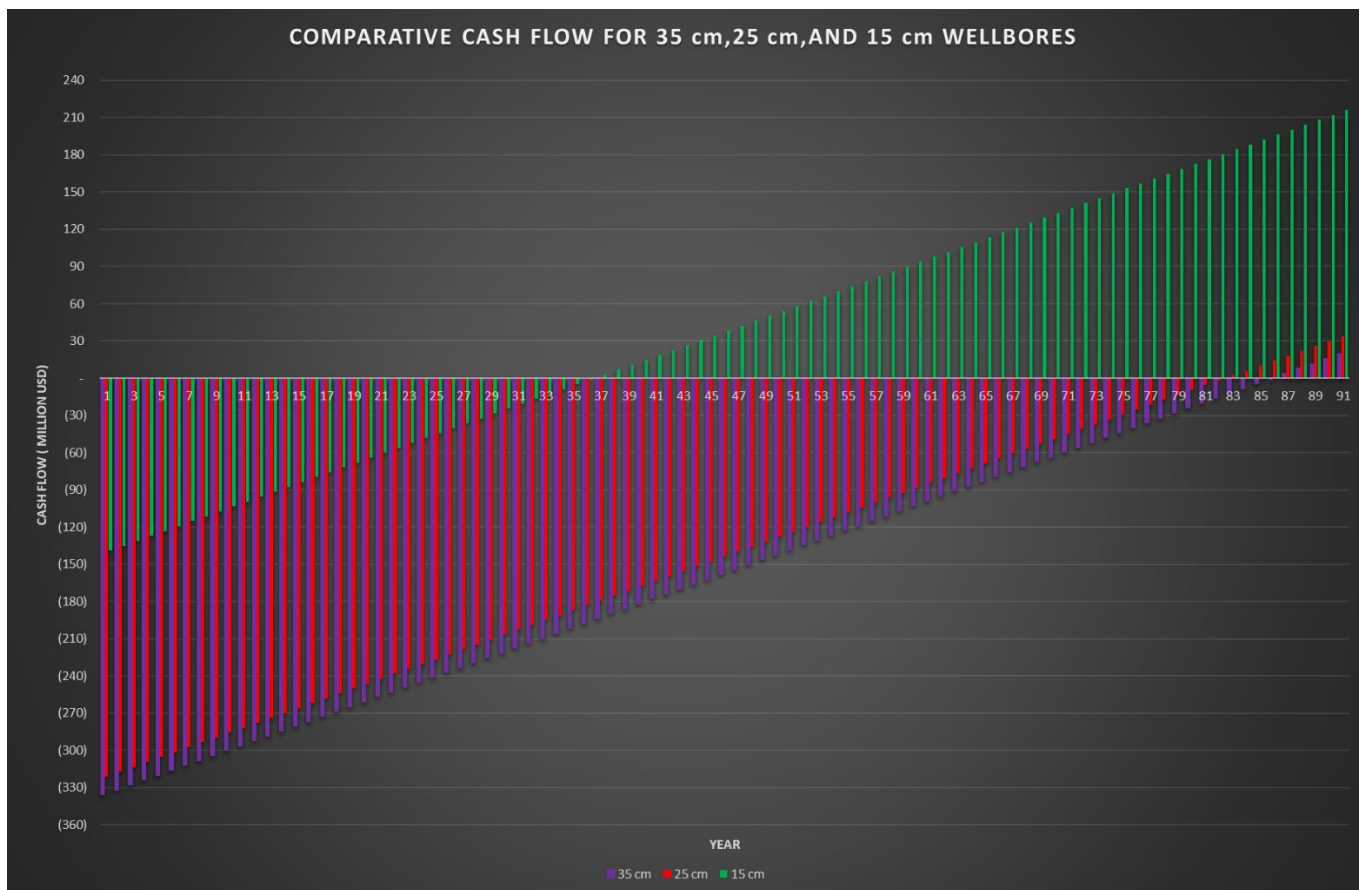
Figure 26: Cash flow for 15cm slim well against full-size wellbore diameters.

Considering a geothermal field such as Ngozi, where a decision is to be made to either use slim wells (15 cm well bore diameter) or full size well (either 25 cm or 35 cm wellbore diameter). It can be observed from the figure 26 above that it takes approximately 36 years using the 15 cm wellbore and binary technology to break even. It can also be observed that if 25 cm full size wells are used instead of slim wells, it will take around 82 years to break even. Moreover if 35 cm wellbore diameters are used, it will take over 86 years to break even.

It takes a relatively long time before the breakeven point is reached, although full size wells take twice the time to break even compared to 15 cm slim well. This partly highlights the importance of government support in terms of grants, subsides or tax exemption in these early phases of project development.

5   CONCLUNSION

This study concludes that if a geothermal field is liquid dominated and low enthalpy, slim wells would be more suitable for the power production instead of full-size wells. The analysis shows that slim wells offer cheaper alternative to full size wells in whatever power cycle technology used, whether single flash, double flash, or binary flash in this kind of geothermal prospect. Also, it can be concluded that in liquid dominated, low enthalpy geothermal fields, where a decision is to be made to drill slim wells, 15 cm well bore diameter slim wells are the most suitable. It has also been shown that it takes less time to break even when slim wells are used to produce power compared to full size wells.

Operation costs for operating a geothermal field with slim wells could prove to be higher than operating full size wells. However, if he chemistry of the fluid is good, with very little or no scaling, slim wells could be more desirable than full size wells. If the field has high scaling potential, then a lot of well workovers will be required due to the small diameters of slim wells. This will increase operational costs compared to full size wells.

Slim wells use modular units to produce power. Many modular units may require more people for operation and maintenance. If slim wells are selected for implementation on power project, then more automated modular power plants would be feasible, and well head technology should be considered to minimize labour power. However, in places where the cost of labour is significantly low, or the project would be required to offer more opportunities for employment then there is no need to be too sophisticated.

It is easier to control load capacity in the grid when using slim wells. Since slim wells use modular units. In developing countries where grid systems are still being improved, it is very complicated to have unplanned maintenance or emergency shut down for units that produce a huge number of megawatts say 30 MW turbine units as this would causes tripping of the grid. Also, sudden outages can cause political and contractual issues. These problems can therefore be minimized if slim wells with modular power plants are used for production.

This study is far from conclusive on the study of power production and cost minimization using slim wells compared to full size wells. Further studies can be considered using organic fluids other than isopentane, which has been used in this thesis.

6   REFERENCES

[1] Parada, A.F.M., 2016: *Phases of geothermal development. Presented at "SDG Short Course I on Sustainability and Environmental Management of Geothermal Resource Utilization and the role of Geothermal in Combating Climate Change", organized by UNU-GTP and LaGeo, Santa Tecla, El Salvador,* 5 pp.

[2] Steingrímsson, B., 2009: *Geothermal exploration and development from a hot spring to utilization. Presented at "Short Course on Surface Exploration for Geothermal Resources", organized by UNU-GTP and LaGeo, Ahuachapán and Santa Tecla, El Salvador,* 5 pp.

[3] International Energy Agency (IEA)., 2020: *Renewables 2020: Analysis and forecast to 2025.* International Energy Agency (IEA), Paris, France. 172 pp.

[4] Climate Majority Project., 2019: *Net-zero by 2050: Investor risk and opportunities in the context of deep decarbonization of electricity generation.* Climate Majority Project, Australia. 20 pp.

[5] Energy Sector Management Assistance Program (ESMAP)., 2012: *Geothermal handbook: planning and financing power generation.* Energy Sector Management Assistance Program (ESMAP), Washington, USA. 164 pp.

[6] Tanzania Invest., 2021: TanzaniaInvest.com, website: https://www.tanzaniainvest.com/power (Accessed May 07, 2021).

[7] Energy Charter Secretariat., 2015: *Tanzania energy sector under the universal principles of the energy charter.* Energy Charter Secretariat, Brussels, Belgium. 70 pp.

[8] International Renewable Energy Agency (IRENA)., 2017: *Renewable's readiness assessment: United republic of Tanzania.* International Renewable Energy Agency (IRENA), Abu Dhabi, United Arab Emirates. 68 pp.

[9] Kajugus, S., Kato, T. K., and Mnjokava, T. T., 2020: Geothermal development in Tanzania. *Proceedings of 8th African Rift Geothermal Congress*, *Nairobi, Kenya,* 13 pp.

[10] Alexander, K. B., Cumming, W., and Marini, L., 2016: Technical review of geothermal potential of Ngozi and Songwe geothermal prospects, Tanzania. *Proceedings of 6th African Rift Geothermal Congress*, *Addis Ababa, Ethiopia,* 11 pp.

[11]   Kalimbia, C., 2016: Business case of Ngozi geothermal power project, Mbeya, SW-Tanzania. Report 21 in: *Geothermal Training in Iceland 2016.* UNU-GTP, Iceland, 359-394.

[12] Adityatama, D., 2020: Slim Hole Drilling Overview for Geothermal Exploration in Indonesia: Potential and Challenges. *Proceedings of the 45th Workshop on Geothermal Reservoir Engineering, Stanford University, California,* 13 pp.

[13] Thórhallsson, S., and Gunnsteinsson, S.S., 2012: Slim wells for geothermal exploration, *presented at "Short Course on Geothermal Development and Geothermal Wells", organized by UNU-GTP and LaGeo, Santa Tecla, El Salvador,* 8 pp.

[14] Mackenzie, G.N.H., Ussher, R.B., Libbey, P.F., et al., 2017: Use of deep slim hole drilling for geothermal exploration, *Proceedings the 5th Indonesia international geothermal convention and exhibition, Jakarta Convention Centre, Indonesia, 19 pp*

[15] Nielson, D.L., Gary, S.K., and Goranson, C., 2017: Slim hole drilling and testing strategies. *Proceedings, 6th ITB International Geothermal Workshop 2017, Institute Technology Bandung, Indonesia,* pp 6

[16] Finger, J., Jacobson, R., Hickox, C., Combs, J., Polk, G., and Goranson, C., 1999: *Slim hole Handbook: Procedures and recommendations for slim hole drilling and testing in geothermal exploration.* Sandia National Laboratories, Albuquerque, NM, Sandia report SAND 99-1976.

[17] Mackenzie, G.N.H., Ussher, R.B., Libbey, P.F., et al., 2017: Use of deep slim hole drilling for geothermal exploration, *Proceedings the 5th Indonesia international geothermal convention and exhibition, Jakarta Convention Centre, Indonesia, 19 pp*

[18] Combs, J. and Gary, G. K., 2000: Discharge capability and geothermal reservoir assessment using data from slim holes. *Proceedings of the World Geothermal Congress 2000, Kyushu-Tohoku, Japan. 6 pp.*

[20] Garg, S. K. and Combs, J., 1993: *Use of slim holes for geothermal exploration and reservoir assessment: A preliminary report on Japanese experience.* Sandia National Laboratories, New Mexico, California, SAND93-7029, 35 pp.

[21] Hosein, R., Serrattan, S., and Jupiter, A., 2018: The viability of slim hole drilling onshore Trinidad. *Journal of Petroleum Exploration and Production Technology, Vol 9, no.2,* 1307-1322 pp.

[22] Finger, J. and Jacobson, R., 2000: Slim hole drilling, logging, and completion technology. *Proceedings of the World Geothermal Congress 2000, Kyushu-Tohoku, Japan. 5 pp.*

[23] Kjartansson, K.D., 2011: *Effect of Well Diameter on Productivity of High Temperature Geothermal Wells.* Faculty of Industrial Engineering, Mechanical Engineering and Computer Science-University of Iceland, Iceland, MSc thesis, 57 pp.

[24] Lubuva, J., 2018: Design of slim well drilling programme for geothermal exploration: case of Ngozi, Tanzania. Report 19 in: *Geothermal Training in Iceland 2016.* UNU-GTP, Iceland, 210-232.

[25]   Pritchett, J. W., 1993: *Preliminary Study of Discharge Characteristics of Slim Holes Compared to Production Wells in Liquid-Dominated Geothermal Reservoirs.* Sandia National Laboratories, New Mexico, California, SAND93-7028, 59 pp.

[26]   Rajput, R.K., 2010: *Engineering Thermodynamics.* Laxmi Publications (P) Ltd, Boston, United States of America, 966 pp.

[27]   DiPippo, R., 2012: *Geothermal power plants: principles, applications, case studies, and environmental impact*, 3rd ed. Butterworth-Heinemann, Amsterdam, 587 pp.

[28]   Saemundsson, K., 2009: Geothermal Systems in Global Perspective, *presented at "Short Course IV on Exploration for Geothermal Resources", organized by UNU-GTP, KenGen and GDC, Lake Naivasha, Kenya,* 11 pp.

[29]   Yılmaz, C., 2018: Comparison of thermo economic cost calculation for a binary geothermal power plant. *Journal of Thermal Engineering, Vol 4, no.5,* 2355-2370 pp.

[30]   Bina, S. M., Jalilinasrabady, S., and Fujii, H., 2017: Thermo-Economic Evaluation and Optimization of a Regenerative ORC Cycle Utilizing Geothermal Energy. *Geothermal Resources Council, Transactions, Vol. 41,* 14 pp.

[31]   World Weather Online: Mbeya monthly averages,2021: *WorldWeatherOnline.com* https://www.worldweatheronline.com/mbeya-weather/mbeya/tz.aspx(accessed Oct. 09, 2020).

[32]   Uhorakeye T., 2008: *Feasibility design of an integrated single-flash binary pilot power plant in NW-Rwanda and drilling of a geothermal well.* UNU-GTP, Iceland, report 27, 20 pp.

[33]   Salas J. R. E., 2014: Feasibility study: cost estimation for geothermal development. *Presented at "Short Course on Surface Exploration for Geothermal Resources", organized by UNU-GTP and LaGeo, Santa Tecla, El Salvador,* 15 pp.

[34]   Mereto, A., 2016: *Thermo economic analysis of geothermal power cycles for IDDP-1 chloride mitigation.* School of Science and Engineering, -Reykjavik University, Iceland, MSc thesis, 92 pp.

[35]   Gunnlaugsson E., et al., 2014: Problems in geothermal operation – scaling and corrosion. *Presented at "Short Course VI Utilization of Low and Medium-Enthalpy Geothermal Resources and Financial Aspects of Utilization", organized by UNU-GTP and LaGeo, Santa Tecla, El Salvador,* 18 pp.

[36]   Mokarram, N.H., and Mosaffa, A. H., 2020: Investigation of the thermo economic improvement of integrating enhanced geothermal single flash with trans critical organic Rankine cycle. *Journal of Energy Conversion and Management, Vol 213, no.112831,* 13 pp.

[37]   Bejan, A., Tsatsaronis, G., and Moran, M. J., 1996: *Thermal design, and optimization.* John Wiley & Sons, New York, 558 pp.

[38]   Zhao, Y., and Wang, J., 2016: Exergo-economic analysis and optimization of a flash-binary geothermal power system. *Journal of Applied Energy, Vol 179,* pp. 159-170.

[39]   Lemmens, S., 2016: Cost Engineering Techniques and Their Applicability for Cost Estimation of Organic Rankine Cycle Systems. *Journal of Energies, Vol 9, no.7*, p. 485

[40]   Bina, S. M., Jalilinasrabady, S., and Fujii, H., 2017: Thermo-Economic Evaluation and Optimization of a Regenerative ORC Cycle Utilizing Geothermal Energy. *Geothermal Resources Council, Transactions, Vol. 41,* 14 pp.

[41]   Maheswari, G. U., et al., 2020: Thermo economic investigation on advanced Kalina power generation system. *Journal of Energy Reports, Vol 6,* pp. 2697–2712

[42]   Pourpasha, H., et al., 2020: Thermodynamic and thermo economic analyses of a new dual-loop organic Rankine – Generator absorber heat exchanger power and cooling cogeneration system. *Journal of Energy Conversion and Management, Vol 224, no.113356*, 13 pp.

[43]   Sinaga, R. H. M., and Darmanto, P. S., 2016: Energy Optimization Modelling of Geothermal Power Plant (Case Study: Darajat Geothermal Field Unit III). *Proceedings, 5th ITB International Geothermal Workshop 2016, Institute Technology Bandung, Indonesia,* 15 pp.

[44]   Velasquez, B., 2016: *Thermo economic analysis and Optimization of Geothermal Power Cycle Utilizing Aqueous Potassium Carbonate for scrubbing Superheated Steam.* Iceland School of Energy, Reykjavik University, Iceland, MSc thesis, 85 pp.

[45]   Couper, J.R., et al., 2012: *Chemical Process Equipment Selection and Design.* Butterworth-Heinemann, Amsterdam, 802 pp.

[46]   Nelson Obert Compressibility Charts, 2021: *eon.sdsu.edu*, website: https://energy.sdsu.edu/testhome/tablesModule/tablesRG/zNO.html

[47]   Yilmaz, C., Kanoglu, M., and Abusoglu, A., 2020: Thermo economic cost evaluation of hydrogen production driven by binary geothermal power plant. *Journal of Geothermics, Vol 57,* pp. 18–25

[48]   Bauner, D., et al., 2012: *Sustainable Energy Markets in Tanzania.* Stockholm Environmental Institute, Stockholm, report no. I, 89 pp.

APPENDIX A

COST RATES IN SINGLE FLASH

Flow of costs in a single flash cycle from the geothermal well to reinjection well including the cost of a unit of power for different wellbore diameters, hence different wellbore characteristics:

m1=30 kg/s; P1=4.94 bar; h1=743.9 kJ/kg.

Stream	c($/kJ)	C($/s)
1		
2		
3		
4		
5		
6		
cwt = 9.1489e-05 $/kJ		

m1=32 kg/s; P1=8.58 bar; h1= 912.28kJ/kg.

Stream	c($/kJ)	C($/s)
1	2.6586e-05	0.14358
2	2.9221e-05	0.14358
3	2.9228e-05	0.090887
4	2.924e-05	0.052699
5	2.9228e-05	0.039748
6	2.9228e-05	0.0014494
cwt =6.3563e-05 $/kJ		

m1=34kg/s; P1=10.19bar; h1= 982.5 kJ/kg.

Stream	c($/kJ)	C($/s)
1	2.1768e-05	0.14358
2	2.3847e-05	0.14358
3	2.3852e-05	0.093189
4	2.3863e-05	0.050397
5	2.3852e-05	0.03862
6	2.3852e-05	0.0014181
cwt =5.5038e-05 $/kJ		

m1=40kg/s; P1=11.58 bar; h1= 1037.2 kJ/kg.

Stream	c($/kJ)	C($/s)
1	1.6743e-05	0.14358
2	1.8294e-05	0.14358
3	1.8297e-05	0.094871
4	1.8306e-05	0.048716
5	1.8297e-05	0.037835
6	1.8297e-05	0.0013965
cwt =4.6061e-05 $/kJ		

m1=47.77 kg/s; P1=12.7bar; h1= 1060.8kJ/kg.

Stream	c($/kJ)	C($/s)
1	5.366e-05	0.57431
2	5.8394e-05	0.57431
3	5.8403e-05	0.37762
4	5.8426e-05	0.19671
5	5.8403e-05	0.1466
6	5.8403e-05	0.0054309
cwt =9.3859e-05 $/kJ		

m1=54 kg/s; P1=13.18 bar; h1= 1066.7 kJ/kg.

Stream	c($/kJ)	C($/s)
1	4.6907e-05	0.57431
2	5.0943e-05	0.57431
3	5.0951e-05	0.37542
4	5.0971e-05	0.19891
5	5.0951e-05	0.1442
6	5.0951e-05	0.00535
cwt = 8.3876e-05 $/kJ		

APPENDIX B

COST RATES IN DOUBLE FLASH

Flow of costs in a double flash cycle from the geothermal well to reinjection well including the cost of a unit of power for different wellbore diameters, hence different wellbore characteristics:

m1=30 kg/s; P1=4.94 bar; h1=743.9 kJ/kg.

Stream	c($/kJ)	C($/s)
1	4.2559e-05	0.14358
2	4.7638e-05	0.14358
3	4.7648e-05	0.08822
4	4.7664e-05	0.055372
5	4.7648e-05	0.063547
6	5.1537e-05	0.055372
7	5.1537e-05	0.026656
8	5.1537e-05	0.028719
9	4.8735e-05	0.090203
10	4.8735e-05	0.069999
11	4.8735e-05	0.0023611
cwt_HPT = 9.5749e-05$/kJ; cwt_LPT = 8.9399e-05$/kJ		

m1=32 kg/s; P1=8.58 bar; h1= 912.28kJ/kg.

Stream	c($/kJ)	C($/s)
1	2.6572e-05	0.14358
2	2.9205e-05	0.14358
3	2.9212e-05	0.09085
4	2.9226e-05	0.052743
5	2.9212e-05	0.053914
6	3.4799e-05	0.052743
7	3.4799e-05	0.033807
8	3.48e-05	0.018939
9	3.1139e-05	0.087721
10	3.1139e-05	0.068224
11	3.1139e-05	0.0023294
cwt_HPT = 6.5453e-05 $/kJ; cwt_LPT = 6.7071e-05 $/kJ		

m1=34kg/s; P1=10.19bar; h1= 982.5 kJ/kg.

Stream	c($/kJ)	C($/s)
1	2.1758e-05	0.14358
2	2.3835e-05	0.14358
3	2.384e-05	0.093158
4	2.3853e-05	0.050436
5	2.384e-05	0.052355
6	2.9325e-05	0.050436
7	2.9326e-05	0.034129
8	2.9327e-05	0.01631
9	2.574e-05	0.086485
10	2.574e-05	0.067314
11	2.574e-05	0.0023081
cwt_HPT =5.6577e-05$/kJ; cwt_LPT = 5.9851e-05$/kJ		

m1=40kg/s; P1=11.58 bar; h1= 1037.2 kJ/kg.

Stream	c($/kJ)	C($/s)
1	1.6736e-05	0.14358
2	1.8285e-05	0.14358
3	1.8289e-05	0.094843
4	1.83e-05	0.048753
5	1.8289e-05	0.051271
6	2.3046e-05	0.048753
7	2.3046e-05	0.034141
8	2.3049e-05	0.014616
9	1.9934e-05	0.085412
10	1.9934e-05	0.066518
11	1.9934e-05	0.0022881
cwt_HPT =4.7393e-05 $/kJ; cwt_LPT =5.1664e-05 $/kJ		

m1=47.77 kg/s; P1=12.7bar; h1= 1060.8kJ/kg.

Stream	c($/kJ)	C($/s)
1	5.3639e-05	0.57431
2	5.8369e-05	0.57431
3	5.8378e-05	0.37751
4	5.8403e-05	0.19683
5	5.8378e-05	0.19859
6	7.4847e-05	0.19683
7	7.4846e-05	0.14092
8	7.4845e-05	0.055909
9	6.4246e-05	0.33951
10	6.4246e-05	0.26448
11	6.4246e-05	0.0091124
cwt_HPT =9.3903e-05 $/kJ; cwt_LPT =9.4050e-05 $/kJ		

m1=54 kg/s; P1=13.18 bar; h1= 1066.7 kJ/kg.

Stream	c($/kJ)	C($/s)
1	4.6889e-05	0.57431
2	5.0921e-05	0.57431
3	5.093e-05	0.37531
4	5.0951e-05	0.19903
5	5.093e-05	0.19531
6	6.5758e-05	0.19903
7	6.5757e-05	0.1437
8	6.5757e-05	0.055335
9	5.6312e-05	0.33901
10	5.6312e-05	0.26412
11	5.6312e-05	0.009104
cwt_HPT = 8.4019e-05 $/kJ; cwt_LPT = 8.4976e-05 $/kJ		

COST RATES IN BINARY FLASH

Flow of costs in a binary cycle from the geothermal well to reinjection well including the cost of a unit of power for different wellbore diameters, hence different wellbore characteristics:

m1=30 kg/s; P1=4.94 bar; h1=743.9 kJ/kg.

Stream	c($/kJ)	C($/s)
1	4.2559e-05	0.14358
2	4.2559e-05	0.028182
3	4.2559e-05	0.013578
10	5.6393e-05	0.15203
11	4.2224e-05	0.035083
12	5.6393e-05	0.075038
13	5.6393e-05	0.018291
14	5.712e-05	0.019888
cwt = 9.2543e-05 $/kJ		

m1=32 kg/s; P1=8.58 bar; h1= 912.28kJ/kg.

Stream	c($/kJ)	C($/s)
1	2.6572e-05	0.14358
2	2.6572e-05	0.033867
3	2.6572e-05	0.0093531
10	3.1303e-05	0.15416
11	2.3084e-05	0.042844
12	3.1303e-05	0.0627
13	3.1303e-05	0.01441
14	3.3111e-05	0.017428
cwt = 5.7533e-05 $/kJ		

m1=34kg/s; P1=10.19bar; h1= 982.5 kJ/kg.

Stream	c($/kJ)	C($/s)
1	2.1758e-05	0.14358
2	2.1758e-05	0.034631
3	2.1758e-05	0.0082567
10	2.4455e-05	0.15533
11	1.744e-05	0.044732
12	2.4455e-05	0.060177
13	2.4455e-05	0.013549
14	2.6697e-05	0.017345
cwt = 4.7888e-05 $/kJ		

m1=40kg/s; P1=11.58 bar; h1= 1037.2 kJ/kg.

Stream	c($/kJ)	C($/s)
1	1.6736e-05	0.14358
2	1.6736e-05	0.035152
3	1.6736e-05	0.0075649
10	1.8152e-05	0.15681
11	1.2668e-05	0.046587
12	1.8152e-05	0.058767
13	1.8152e-05	0.013025
14	2.076e-05	0.017835
cwt = 3.8908e-05 $/kJ		

m1=47.77 kg/s; P1=12.7bar; h1= 1060.8kJ/kg.

Stream	c($/kJ)	C($/s)
1	5.3639e-05	0.57431
2	5.3639e-05	0.14582
3	5.3639e-05	0.029243
10	5.4721e-05	0.60733
11	3.6001e-05	0.17686
12	5.4721e-05	0.22254
13	5.4721e-05	0.048759
14	5.4383e-05	0.058962
cwt = 7.6760e-05 $/kJ		

m1=54 kg/s; P1=13.18 bar; h1= 1066.7 kJ/kg.

Stream	c($/kJ)	C($/s)
1	4.6889e-05	0.57431
2	4.6889e-05	0.14874
3	4.6889e-05	0.029019
10	4.7369e-05	0.60794
11	3.1233e-05	0.18027
12	4.7369e-05	0.22082
13	4.7369e-05	0.048161
14	4.746e-05	0.059112
cwt = 6.7971e-05 $/kJ		

School of Science and Engineering
Reykjavik University
Menntavegur 1
101 Reykjavik, Iceland
Tel. +354 599 6200
Fax +354 599 6201
www.ru.is